HHS Public Access

Author manuscript

Cancer Gene Ther. Author manuscript; available in PMC 2013 January 01.

Published in final edited form as:

Cancer Gene Ther. 2012 July ; 19(7): 476–488. doi:10.1038/cgt.2012.23.

Peptide Targeting of Adenoviral Vectors to Augment Tumor Gene Transfer

Erin N. Ballard, **Van T. Trinh**, **Richard T. Hogg**, and **Robert D. Gerard**

University of Texas Southwestern Medical Center, Department of Internal Medicine, 6000 Harry Hines Blvd. NB10.218A, Dallas, TX 75390-8573, Tel 214-648-4997, Fax 214-648-1450

Abstract

Adenovirus serotype 5 remains one of the most promising vectors for delivering genetic material to cancer cells for imaging or therapy, but optimization of these agents to selectively promote tumor cell infection is needed to further their clinical development. Peptide sequences that bind to specific cell surface receptors have been inserted into adenoviral capsid proteins to improve tumor targeting, often in the background of mutations designed to ablate normal ligand:receptor interactions and thereby reduce off target effects and toxicities in non-target tissues. Different tumor types also express highly variable complements of cell surface receptors, so a customized targeting strategy using a particular peptide in the context of specific adenoviral mutations may be needed to achieve optimal efficacy. To further investigate peptide targeting strategies in adenoviral vectors, we used a set of peptide motifs originally isolated using phage display technology that evince tumor specificity *in vivo*. To demonstrate their abilities as targeting motifs, we genetically incorporated these peptides into a surface loop of the fiber capsid protein to construct targeted adenovirus vectors. We then systematically evaluated the ability of these peptide targeted vectors to infect several tumor cell types, both *in vitro* and *in vivo*, in a variety of mutational backgrounds designed to reduce CAR and/or HSG-mediated binding. Results from this study support previous observations that peptide insertions in the HI loop of the fiber knob domain are generally ineffective when used in combination with HSG detargeting mutations. The evidence also suggests that this strategy can attenuate other fiber knob interactions, such as CAR-mediated binding, and reduce overall viral infectivity. The insertion of peptides into fiber proved more effective for targeting tumor cell types expressing low levels of CAR receptor, as this strategy can partially compensate for the very low infectivity of wild-type adenovirus in those cells. Nevertheless, the incorporation of relatively low affinity peptide ligands into the fiber knob, while effective *in vitro*, has only minimal targeting efficacy *in vivo* and highlights the importance of high affinity ligand:receptor interactions to achieve tumor targeting.

Keywords

peptide; adenovirus; targeting; integrin; tumor; aminopeptidase N

Correspondence to: Robert D. Gerard.

Supplementary information is available at the Cancer Gene Therapy's website.

Introduction

Human adenovirus serotype 5 (Ad5) remains one of the most studied vectors for gene therapy applications based on its capacity to accommodate large DNA insertions and the ability to infect both dividing and quiescent cells with high efficiency. These agents have been extensively developed for delivering transiently expressed transgenes to solid tumors for imaging and therapeutic applications, but they infect a broad range of cell types because of widespread distribution of primary cell surface receptors used by wild-type Ad5. While this characteristic has helped facilitate their development as gene delivery vehicles, this promiscuous behavior can decrease their effectiveness and result in potentially dangerous toxicities due to immune and inflammatory responses. More than 99% of systemically administered wild-type Ad5 is taken up by the liver, potentially resulting in severe hepatic dysfunction.[1–4] The primary mode of adenoviral infection involves binding of the adenoviral fiber knob to the coxsackievirus and adenovirus receptor (CAR)[5] followed by interactions between the penton base Arg–Gly–Asp (RGD) motif with cellular integrins αvβ3 and αvβ5 to promote internalization of the virus.[6] Ablating CAR and integrin-mediated interactions have been shown to reduce liver transduction in some studies, but others show mixed results.[7–10] Since many tumor cells also express high levels of surface integrins and low levels of CAR, removing the RGD motif in the penton base to reduce native interactions may not be a rational strategy for vectors designed to target cancer cells.

Studies also indicate that CAR and integrin-mediated interactions are unlikely to be the primary mechanisms of liver infection, based on high residual levels of *in vivo* liver transduction following ablation of CAR or integrin-mediated binding.[11] Indeed, recent studies have shown that hexon-coagulation factor interactions are responsible for much of the liver transduction. [12–14] However, interactions between the KKTK sequence in the adenoviral fiber shaft and heparin sulfate glycosaminoglycans (HSGs) can be important for liver infection, [15, 16] and efforts to detarget Ad vectors from their native interactions through mutation of the CAR and HSG binding sites in the fiber knob and fiber shaft, respectively, can reduce liver gene transfer *in vivo* by nearly two orders of magnitude in both mice and non-human primates.[10, 17, 18] Recent work in our lab has shown similar reductions in liver infection for CAR and HSG detargeted vectors in tumor-bearing mice, [19] but these mutations also reduced tumor infectivity and resulted in no improvement in overall tumor specificity for these vectors as compared to wild type. The overall reduction in liver infection, however, means that adenoviral vectors with ablated CAR and/or HSG binding could be good platforms for introducing further modifications to increase tumor cell infection and improve tumor specificity.

A variety of techniques have been evaluated for retargeting adenoviral vectors to tumor cells. One promising strategy involves the insertion of ligands into the exposed surface HI-loop of the Ad5 capsid, using various peptide sequences identified using phage display that specifically target tumor vasculature.[20] The RGD sequence in the cyclic peptide CDCRGDCFC is a selective binder of αvβ3 and αvβ5 integrins which has been shown to direct binding to tumor vasculature.[21, 22] Additional peptide sequences that can be used to target either tumors or tumor vasculature include the asparagine-glycine-arginine (NGR) cell adhesion motif that specifically binds aminopeptidase N (APN/CD13), an enzyme that is

minimally expressed on normal endothelium but is markedly up-regulated in tumor neovasculature.[23, 24] A motif containing glycine-serine-leucine (GSL) was also recovered from phage display screening of breast carcinomas and other tumor types,[25] although further work is needed to evaluate this motif and the derivative alanine-serine-leucine (ASL) that we utilized for their ability to target tumor cells and the nature of the receptor bound by this ligand. RGD and NGR motifs, however, have been evaluated in a variety of systems for targeting tumors.[25–28] Both of these peptide motifs have also been incorporated into capsid proteins for retargeting adenoviral vectors to tumors or tumor vasculature. The NGR motif has been shown to increase the ability of adenoviral vectors to transduce tumor cells *in vitro*,[29–31] and minimally augmented *in vivo* tumor transduction has been accomplished using intratumoral delivery of these vectors.[31] Incorporating an RGD motif has also improved tumor cell transduction by adenovirus in a variety of *in vitro* studies, although this approach has had mixed results *in vivo*.[10, 32–34]

Implementation of peptide targeting strategies must be performed cautiously because the deletion of native peptide sequences or the incorporation of novel targeted peptides could have dramatic effects on the biodistribution and/or stability of adenoviral vectors.[35] In fact, recent studies suggest that ablation of the HSG binding site in the fiber shaft reduces the efficacy of peptide retargeting motifs incorporated into the adenoviral fiber knob, either because structural changes in the fiber reduce the accessibility of the peptide ligand or because mutations in the KKTK sequence reduce liver transduction by an unknown mechanism following primary receptor binding by liver cells.[10, 36] These studies suggest that retargeting adenoviral vectors using HI peptide insertions in the context of CAR and HSG detargeting might be ineffective for improving tumor specific infection. Another study showed that a RGD motif inserted in the HI loop failed to retarget adenovirus to tumors in a mouse xenograft model when the KKTK motif was mutated to ablate HSG interactions,[10] but this group did not assess whether peptide ligands could retarget vector when HSG interactions were left intact. The biodistribution of adenoviral vectors incorporating HI loop peptide insertions in the context of various detargeting strategies is therefore still in question.

In this study, we further investigate the use of tumor-targeting peptide motifs for reducing liver infection and improving the tumor specificity of adenoviral vectors both *in vitro* and *in vivo*. We evaluate this strategy using a variety of retargeting peptides inserted into the HI loop of the adenoviral fiber knob domain, either with or without ablation of CAR binding, HSG binding, or both. The goal of this investigation is to further assess the feasibility of peptide retargeting and to identify optimal vector platforms for the insertion of peptide targeting ligands in the adenoviral fiber HI loop for cancer imaging and therapy.

Materials and Methods

Adenoviral expression vectors

Peptide retargeted vectors were constructed by first introducing a *Bsp*E1 restriction site at ^{542}TG^{543} of the fiber gene in pQE30Ad5Knob using the QuickChange® mutagenesis protocol (Stratagene, La Jolla, CA). Mutations in the CAR binding site of the pQE30Ad5Knob expression vector and mutations in the pFiber (a plasmid containing Ad5

np#30818-33306) HSG binding site were produced to modify residues in the fiber gene previously shown to be involved in native CAR and HSG interactions.[17, 18, 37] ^{417}KDAK^{420} in fiber knob was mutated to either ^{417}QDAD^{420} or ^{417}GDAA^{420} to ablate CAR interactions, and ^{91}KKTK^{94} at the end of the third repeat in the fiber shaft was mutated in pFiber to ^{91}EAGA^{94} to reduce HSG-mediated interactions. Oligonucleotides encoding the peptides of interest were ligated into pQE30Ad5Knob following cleavage with *Bsp*E1. Oligos were designed so that properly oriented constructs could be identified by *Bsp*E1 digestion. Targeting peptide sequence insertions were GGCDC**RGD**CFCG, GG**NGR**AHAS, and GGC**ASL**VRCG.

Oligos used for peptide insertions were as follows:

RGD(fwd):CCGGTGGTTGTGATTGC**CGTGGTGAT**TGCTTCTGTGGCT;

RGD(rev):CCGGAGCCACAGAAGCA**ATCACCACG**GCAATCACAACCA;

NGR(fwd):CCGGTGGT**AACGGTCGT**GCTCATGCATCTT;

NGR(rev): CCGGAAGATGCATGAGC**ACGACCGTT**ACCA;

ASL(fwd): CCGGTGGTTGT**GCTTCTCTG**GTACGCTGTGGTT;

ASL(rev): CCGGAACCACAGCGTAC**CAGAGAAGC**ACAACCA.

Mutated knob domains were moved from the pQE30 expression vector into pFiber, and the entire fiber gene was sequenced to verify the mutations and proper peptide insertions. These fiber mutations were subsequently incorporated into the recombinant viral genome cloned into pTG3602CMVlux (pTG3602 containing a luciferase transgene under the control of the human CMV immediate early promoter inserted into the viral E1 region) using homologous recombination in *E. coli* BJ5183.[38] Virus was reconstructed from the plasmid by excising the viral genome with *Pac*I and transfection into 911 cells using Lipofectamine 2000 (Invitrogen, Carlsbad, CA).

Purified virus preparation

Viruses that were not mutated for HSG and CAR interactions were propagated and purified as previously described.[39] Briefly, large-scale preparations were grown on 911 cells, harvested and purified sequentially on CsCl step gradients and Sepharose CL-4B columns equilibrated with Tris-buffered isotonic saline (137mM NaCl, 5mM KCl, 10mM Tris-HCl pH7.4, 1mM $MgCl_2$). For adenoviral vectors with HSG and/or CAR binding mutations, propagation exclusively in 911 cells is possible, but extremely slow due to poor infectivity of the mutated virus. The wild-type Ad5 fiber complementing cell line 633 was kindly provided by Dr. Glen Nemerow and was therefore used for all initial plaque purification and small scale stock virus propagation.[40] The ultimate propagation of these vectors was performed on 911 cells to yield preparations with only the mutant fiber incorporated into the virion particles, which were subsequently purified as above. Virus concentrations were determined using a spectrophotometer, with 1.0 A_{260} equal to 1.0×10^{12} particles per ml. Viruses were stored frozen at −80°C after the addition of 10% glycerol at concentrations between 10^{12} and 10^{13} particles per ml until use.

Production of soluble fiber knob constructs

Soluble fiber knob proteins including wild-type and those with mutations to ablate CAR interactions were prepared both with and without RGD, NGR, or ASL targeting peptide moieties by expression in *E. coli* SG13009 as a six histidine N-terminal affinity-tagged protein using the commercially available plasmid expression vector pQE30 from Qiagen (Valencia, CA). Expression and purification of the knob protein to homogeneity in mg quantities was carried out in a straightforward manner using IPTG induction, salt/detergent extraction of the soluble knob and affinity purification on a Ni-agarose column according to the supplier's protocols. For CAR− knob variants, expression at 30°C increased the yield of soluble protein. Purified protein was dialyzed versus Tris-buffered isotonic saline containing 10% glycerol and stored frozen at −80°C. SDS-PAGE was used to confirm purity of the preparations.

Cell culture

Permissive 911cells, clonal HT1080 fibrosarcoma cells, DU145 prostate cancer and MDA-MB-435s human melanoma cells (ATCC# HTB-129™, originally thought to be a breast cancer line) were all propagated in Dulbecco's minimal essential medium (DMEM) containing 10% fetal bovine serum (FBS). ES-2 human ovarian carcinoma cells (ATCC# CRL-1978™) were propagated in McCoy's medium with 10%FBS, and CHO K1 cells were propagated in a 50:50 mixture of DMEM:F12 with 10%FBS.

Infections of cells *in vitro* to compare viruses harboring different fiber mutations were performed with purified stocks of viruses diluted into DMEM containing 2% FBS using defined titers (in particles per ml) for infection. Cell cultures were infected for 1 hr at 37°C, and incubated overnight to permit luciferase expression before cells were harvested and luciferase activity determined to assess the level of gene expression as an indicator of infectivity. To assess virus binding and uptake to cells *in vitro* as an independent measure of transduction efficiency, an aliquot of the extract from wells infected with the highest viral concentration used for the luciferase expression assay was collected for quantitative real-time PCR, which was performed as previously described.[41]

Infections of cells *in vitro* to compare the ability of different knob mutants to compete for virus infection were performed as previously described[42] with purified knob proteins (0.1 μg/mL) diluted into DMEM containing 2% FBS and allowed to pre-absorb to cell monolayers for 30 min at room temperature before the addition of virus. After 30 min of virus absorption, cells were washed and incubated overnight at 37°C to allow for luciferase expression and quantification of viral DNA content as described above.

Determination of cell surface integrin expression using quantitative RT-PCR (qRT-PCR)

Relative expression levels of mRNA encoding αv, β3 and β5 integrin subunits in tumor cell lines were assessed using the PrimeTime® qPCR assay (Integrated DNA Technologies, Coralville, IO). For details on experimental protocol, see supplementary material.

Animal experiments

All animal experiments were approved by the Institutional Animal Care and Use Committee. Female mice were used preferentially for HT1080 and MDA-MB-435s tumor cell implantation, although not exclusively. Mice were injected subcutaneously with $3–5\times10^6$ cells suspended in 0.5ml DMEM on the dorsal flank. Tumors were allowed to grow until 0.4–0.8 cc in size as measured by calipers, at which time the various purified adenoviral constructs were injected via the tail vein at doses of $10^{10}–10^{11}$ particles per mouse.

Luciferase Imaging and Biochemical Determination

Three days after injection of adenovirus, mice to be imaged were anaesthetized with isoflurane and injected subcutaneously with luciferin (0.1 mg/g body weight). Whole body luciferase activity was imaged with a Lumina bioluminescence imaging system (Caliper Biosciences, Hopkinton, MA). Total tumor light flux was quantified using the imaging software provided with the instrument. Mice were subsequently sacrificed and major organs and tumors removed for biochemical determination of luciferase activity performed as previously described.[41] Viral DNA content in tissues was measured by real time PCR detection of the adenovirus type 5 hexon gene as previously described.[41]

Statistical Analyses

SigmaStat for Windows v3.11 was used to perform Mann-Whitney Rank Sum Test analyses for pairwise comparisons between individual treatment groups and controls.

Results

Evaluation of cell surface receptor density in various cell lines

The cells used in this study were chosen based on variations in cell surface receptor profiles to evaluate the different contributions of CAR, integrin, and APN/CD13-mediated interactions with the various vectors and peptide retargeting strategies (Table 1). The scientific literature served as a source of some of these data, notably the expression levels of APN/CD13. CAR receptor expression levels were estimated from the relative ability of soluble knob protein to block adenoviral infection and subsequent luciferase transgene expression ([19] and data not shown). DU145 cells expressed very high CAR levels (33,000–53,000 sites per cell) that were determined by Scatchard analysis.[42]

In addition to fiber knob-CAR binding as the primary, high-affinity interaction, Ad5 employs interactions between the RGD motif in the penton base and the αvβ3 and αvβ5 integrins to promote binding and/or viral entry into cells.[43] Incorporation of the RGD peptide into the HI surface loop in the fiber knob was one of the peptide targeting strategies used in this study, so we assessed relative mRNA expression of αv, β3, and β5 integrin subunits in the various cell lines using quantitative RT-PCR. Results indicate that CHO K1 and MDA-MB-435s cells exhibit the highest levels of integrin expression, with ES-2 and HT1080 cells expressing lower levels of integrin subunits (Supplemental Figure 1). Since proangiogenic factors such as VEGF-A and FGF2 have been shown to increase integrin expression, the *in vitro* tumor cell receptor expression profile and vector infectivity is only an approximation of that expected *in vivo* for tumors.

Effect of RGD, NGR, and ASL targeting peptides on infection of various cell lines with HSG-CAR-vectors

To obtain a preliminary assessment of the ability of RGD, NGR and ASL peptide motifs for retargeting Ad vectors, we first used an Ad vector with mutations designed to ablate both CAR and HSG binding (AdH−C−) as the experimental platform. In MDA-MB-435s cells expressing undetectable levels of CAR, insertion of the RGD or NGR peptides into the HI loop resulted in similar or slightly reduced viral infectivity compared to untargeted AdH−C− (Figure 1, panel A). However, insertion of the ASL peptide increased viral infectivity since the concentration of AdH−C−ASL virus needed to achieve similar luciferase expression decreased by a log compared to untargeted AdH−C−. Results similar to those seen on MDA-MB-435s cells were observed for all viruses in CHO K1 and ES-2 cells using the AdH−C− platform (Supplemental Figure 2 and Table II), and comparison of the three peptides showed that ASL>RGD>NGR. In HT1080 tumor cells, incorporation of all peptides improved cell targeting, as shown by a 2–16 fold decrease in the concentration of virus needed to achieve equivalent luciferase expression compared to untargeted AdH−C− (Figure 1, panel B). In HT1080 cells, NGR peptide targeting was more effective than on the other three cell types.

All three cell lines that express either low or no CAR showed comparable expression from AdH−C− and AdH+C+ viruses (Figure 2, panel A, and data not shown). By contrast, since HT1080 cells express CAR, they showed approximately 30-fold greater infectivity by AdH +C+ than AdH−C− (Figure 2, panel B)

Increases in luciferase expression were roughly correlated with improved cell transduction assessed by quantifying cell associated viral DNA using TaqMan qPCR (Table II). Up to 3-fold increases in cell-associated viral DNA were detected for the peptide targeted viruses compared to untargeted virus in tumor cells by quantitative PCR, and the rank order of comparative efficiency is consistent with that seen for luciferase expression.

Effect of RGD, NGR, and ASL targeting peptides on infection of various cell lines with wild-type vectors

Results from prior investigations suggest that mutations in the KKTK HSG binding motif reduce the efficacy of peptide retargeting using an RGD peptide.[10, 36] We therefore tested these peptide motifs in an adenoviral vector platform with intact CAR and HSG binding (AdH+C+). All three targeting peptides improved luciferase expression compared to untargeted AdH+C+ in all cells tested including MDA-MB-435s and HT1080 tumor cells (Figure 1, panels C and D) as well as ES-2 and CHO K1 cells (Supplemental Figure 2, panels C and D). The greatest increases in luciferase expression for the peptide targeted viruses occurred in the CAR-negative cell lines in which 2- to 42-fold decreased concentrations of viruses achieved luciferase expression equal to untargeted AdH+C+ (Table III). In CAR-positive HT1080 cells, improved infectivity was more modest, and ranged from 2- to 4-fold.

Increases in luciferase expression for peptide targeted AdH+C+ vectors again were correlated with increases in cell-associated viral DNA determined by quantitative real time PCR (Table III). However, a greater degree of transduction for all three targeted viruses over

nontargeted AdH+C+ was observed in ES-2 cells. CHO K1 cells also showed anomalously high levels of transduction by the AdH+C+RDG virus that correlated closely with the higher level of reporter gene expression.

Taken together, these data shown that viral transduction and reporter gene expression are not always tightly correlated as is commonly assumed, and this can greatly complicate any analysis of targeting efficacy. In the H+C+ vector backbone, peptide targeting generally resulted in smaller overall increases in viral transduction and gene expression in HT1080 tumor cells than in the three CAR-negative tumor cell lines. In the H−C− vector backbone, increases in viral transduction were more readily apparent in all cell lines, although most changes in transduction or gene expression that occurred as a consequence of peptide insertion into the HI loop of the fiber knob were small and typically amounted to less than an order of magnitude.

Evaluating the effects of individual HSG and CAR mutations on viral infectivity using peptide targeting in vitro

To further analyze the effects of individual mutations on the efficacy of RGD peptide targeting, we next evaluated adenoviral constructs with various combinations of mutations designed to eliminate HSG and/or CAR binding. In CAR-negative MDA-MB-435s cells, the addition of RGD peptide into the singly mutated AdH+C− or AdH−C+ vectors resulted in either no change or a slight reduction in luciferase expression compared to the corresponding vectors lacking the peptide (Figure 2, panel C), although a 4- to 9-fold increase in cell transduction was observed for the RGD targeted vectors (Table IV). Similar results were observed using the CAR-negative CHO K1 and ES-2 cell lines (Supplementary Figure 3). In CAR-positive HT1080 cells, AdH+C−RGD showed very similar levels of luciferase compared to non-targeted AdH+C− (Figure 2, panel D), although a 7-fold increase in viral DNA was detected in cells infected with the RGD targeted vector. Interestingly, the addition of RGD peptide in the AdH−C+ vector dramatically reduced its infectivity in HT1080 cells- a 30-fold higher concentration of AdH−C+RGD was required to reach similar luciferase expression compared to untargeted AdH−C+ (Figure 2, panel D). This suggests that not only is RGD targeting ineffective in the context of HSG mutations, but also that the presence of RGD peptide in the HI loop might attenuate CAR interactions in vectors with ablated HSG interactions.

As shown above, only in the case of the wild type H+C+ vector platform was cell infection increased by incorporation of the RGD peptide. In cells expressing high levels of integrins and low/no CAR, MDA-MB-435s (Figure 2, panel A), CHO K1 and ES-2 (Supplemental Figure 3), substantial increases of 30- to 60-fold in the efficiency of luciferase expression and in viral transduction (5- to 36-fold) were observed (Table IV). In HT1080 cells, RGD peptide insertion into wild-type AdH+C+ fiber resulted in smaller concentration-dependent increases in luciferase expression compared to untargeted control vectors (approximately 2-fold; Figure 2, panel B). This is likely because high affinity fiber knob:CAR interactions dominate the infection process in this CAR-positive cell line, and the addition of low affinity RGD:integrin interactions result in only a small increase in infectivity.

Inhibition of peptide targeting on various cell lines using soluble fiber knob constructs

The fiber knob of adenovirus serotype 5 forms a highly stable trimeric structure that has previously been functionally and structurally characterized,[42, 44] and previous data from our lab showed that a wild-type soluble fiber knob construct reduces infectivity of HT1080 cells up to 90% *in vitro* by binding to CAR and eclipsing virus attachment.[19] To further demonstrate the contributions of native ligand:receptor interactions and the specificity of peptide retargeting strategies in adenoviral vectors, we constructed bacterial expression vectors for wild-type or CAR-negative fiber knob proteins both with and without targeting peptide insertions to be used as soluble, competitive inhibitors of wild-type or peptide targeted adenoviruses.

As expected, in CAR-negative MDA-MB-435s cells, the CAR status of the soluble knob inhibitor protein was irrelevant, as the virus cannot utilize CAR as a receptor (Figure 3). In CAR-positive HT1080 cells, the CAR-positive knob proteins were capable of inhibiting AdH+C+viral transduction, but CAR-negative knob proteins were not. Wild-type CAR+ soluble knob reduced the relative luciferase expression of wild-type virus by approximately 30–40%.

Interestingly, the RGD targeted soluble knob showed additional competition for virus transduction, and only of the RGD targeted viruses. Addition of relatively high concentrations (0.1 mg/ml) of soluble CAR+RGD or CAR−RGD targeted knob significantly reduced luciferase expression due to AdH+C+RGD virus in HT1080 and MDA-MB-435s cells (Figure 3). Similar results were also seen in the CAR-negative CHOK1 cells (Supplemental Figure 4). In HT1080 cells, the competitive effect of the RGD peptide was apparently greater than that of CAR+knob alone (up to 70% inhibition), that may indicate eclipse of integrin receptor binding.

CAR status was the only determinant in the ability of soluble knob competitors to inhibit relative luciferase expression in another cell line (DU145) that has relatively low levels of integrins[45, 46] and very high levels of CAR. RGD and other peptides provided no added competitive effect on any virus in this cell line over that seen with wild type knob (Supplemental Figure 4).

Surprisingly, inhibition of any virus was minimal or nonexistent when NGR or ASL soluble knob constructs were used as competitors in any of the cell lines tested. Any additional infectivity conferred by NGR or ASL peptide on the virus was not competed out by the soluble knob proteins containing those same peptides even when higher concentrations of soluble competitors were used (data not shown). We attribute this to two factors-the multivalent nature of the virus, which contains 12 copies of the fiber protein and is likely a more avid ligand than the soluble knob, and the relatively low affinity of NGR and ASL for their respective receptors.

In summary, peptide targeted knob proteins were ineffective competitors *in vitro*, with the exception of the RGD peptide knob which was able to specifically inhibit RGD-targeted viral infection of a variety of integrin-expressing cells. These data are consistent with the observations made above that high affinity fiber knob:CAR interactions dominate the

infection process in CAR-positive cell lines. The addition of low affinity peptide:receptor interactions only result in observable competition when viral:CAR interactions are lacking.

Effect of peptide retargeting on adenoviral vectors with ablated CAR and HSG interactions in tumor bearing mice

We first assessed the ability of RGD, NGR, and ASL peptide sequences to improve tumor targeting of the double mutated AdH−C− vector in our HT1080 fibrosarcoma mouse model. *In vivo* imaging of luciferase showed that expression was frequently observed in tumors using whole animal bioluminescence (Supplemental Figure 5) for all four H−C− vectors. Expression in other tissues was not observed.

Developing HT1080 fibrosarcomas were also a major target of gene transfer and expression from the AdH−C− vector as shown biochemically by analyzing organ homogenates as previously reported.[19] AdH−C−NGR and AdH−C−ASL showed similar luciferase expression (RLU per mg of tissue) and transduction (viral DNA per mg of tissue) compared to untargeted AdH−C− in both liver and tumor (Figure 4, panels A and B). All other tissues tested including heart, kidney, lung, and spleen (data not shown) showed similar results for the three different viruses. This suggests that inclusion of these peptides had little effect on the biodistribution of the double mutant AdH−C− vector. However, the AdH−C−RGD vector showed significantly reduced luciferase expression (Figure 4, panel A) in both liver (18-fold) and tumor (20-fold) as well as reduced viral transduction (Figure 4, panel B) of the liver (50-fold) compared to untargeted AdH−C−. The 9-fold reduction in tumor transduction approached but did not achieve statistical significance (p=0.071). Luciferase expression was also significantly reduced in the heart, kidney, and lung, and viral DNA per mg of tissue was significantly reduced in the heart, lung, and spleen for AdH−C−RGD compared to AdH−C− (data not shown).

No improvement in tumor specificity as indicated by the tumor/liver ratio of luciferase expression or viral DNA per mg tissue was observed for any of the three targeted viruses as compared to the control (Figure 4, panels A and B). Gene expression per copy of viral DNA delivered to the tissue (Figure 4, panel C) was similar for all three peptide targeted viruses in comparison to the control with one exception. The AdH−C−NGR virus showed a 1-log increase in gene expression per copy of viral DNA delivered in all tissues except liver and lung, which translated into a 9-fold increase in the tumor/liver ratio for this virus.

Effect of peptide targeting on adenoviral vectors with wild type CAR and HSG interactions in tumor bearing mice

Previous studies have suggested that the incorporation of the RGD peptide in the HI loop is ineffective for retargeting adenovirus when mutations are introduced into the fiber shaft to ablate HSG interactions.[10, 36] We therefore compared the *in vivo* infectivity of peptide targeted AdH+C+ vectors with untargeted AdH+C+ in HT1080 tumor bearing mice. The results of in vivo bioluminescent imaging are shown in Supplementary Figure 6. Similar to what we observed previously,[41] a dose of 10^{11} particles per mouse resulted in high levels of expression in both tumor and liver. Injection of peptide targeted viruses clearly reduced overall gene expression detected by optical imaging, and appeared to increase the specificity

of tumor expression in some instances (for example, mice 2717, 2723, 2729 and 2867 in the AdH+C+NGR group). Luciferase expression detected by whole animal imaging was clearly lowest for the AdH+C+RGD group.

However, biochemical analysis of luciferase expression is a more accurate quantitative measurement of gene expression *in vivo*. As was observed for the AdH−C−RGD vector, AdH+C+RGD showed significantly reduced luciferase expression (Figure 5, panel A) in both liver (11-fold) and tumor (20-fold) as well as reduced viral transduction (Figure 5, panel B) of the liver (5-fold) compared to untargeted AdH+C+. There were also no significant changes in tumor/liver ratio for gene expression, gene delivery or luciferase expression per DNA copy (Figure 5, panel C) that were due to RGD peptide incorporation.

Incorporation of the NGR peptide resulted in a small but significant increase in the mean luciferase expression in tumor tissue (in keeping with the results observed by optical detection of bioluminescence), that did not result in any change in the tumor/liver ratio (Figure 5, panel A). This was despite significantly less viral gene delivery to both liver (10-fold) and tumor (7-fold) quantified by PCR (Figure 5, panel B). As a result, the specific activity of expression from the AdH+C+NGR virus in both the liver and tumor were increased and the tumor/liver ratio decreased by a factor of 5. However, the results for specific activity of expression from the AdH+C+NGR virus were probably biased by anomalous values for two mice in the group which skewed the data, so these results should be interpreted cautiously.

The ASL peptide insertion into fiber knob had no effect on luciferase expression *in vivo*, but significantly reduced viral gene delivery in the liver with no discernable effects on gene delivery in tumor (Figure 5, panel B). There was no change in the tumor/liver ratios of luciferase expression, viral gene delivery, or specific activity of gene expression with this virus.

Since MDA-MB-435s cells express much higher levels of integrins and are targeted *in vitro* several fold more efficiently than HT1080 cells by the AdH+C+RGD vector (Table III), we also tested this vector in an *in vivo* MDA-MB-435s flank tumor model. Compared to HT0180 tumors, the MDA-MB-435s tumors were relatively avascular and grew very slowly. *In vivo* bioluminescent imaging of luciferase expression (Supplemental Figure 7) showed that the liver is the primary site of gene expression in most animals at a dose of 10^{11} particles of AdH+C+ with little evidence of tumor expression, as was previously observed for non-tumor-bearing mice. By contrast, liver expression was not seen when AdH+C+RGD was injected into mice. Biochemical analysis of luciferase expression showed no significant differences between the two viruses in either tumor or liver (Figure 6, panel A) or in any other tissue (data not shown). The mean tumor/liver ratio was 11-fold higher for the RGD peptide targeted virus but the difference was not statistically different. Quantification of viral DNA delivery to the tissues by the AdH+C+ and AdH+C+RGD viruses showed a significant 12-fold reduction in the liver but no difference in DNA delivery to the tumor or the tumor/liver ratio (Figure 6, panel B). Apparently, the minimal increases in cell transduction observed *in vitro* for HT1080 and MDA-MB-435s cells are not sufficient to significantly increase *in vivo* tumor specificity for the RGD-targeted virus.

Effect of various mutational backgrounds on adenoviral infectivity and RGD peptide targeting in tumor-bearing mice

We also evaluated the AdH+C− and AdH−C+ singly mutated vectors with and without incorporation of the RGD targeting peptide in the HT1080 *in vivo* tumor model. A summary figure of the effects of all possible mutational backgrounds with and without targeting peptides is shown in Figure 7. With no peptide insertions, single H− or C− mutations had no substantial effect on luciferase expression or cell transduction in liver or tumor, although a small increase in luciferase expression was observed in liver for AdH+C− compared to AdH +C+. Ablation of both H- and C-interactions significantly reduced luciferase expression in both liver and tumor, and also significantly reduced liver cell transduction.

RGD peptide insertion reduced liver transgene expression and transduction in the context of all H- and/or C- mutational backgrounds when compared to untargeted controls, and these effects were significant in all cases except AdH+C− versus AdH+C−RGD (p=0.059). In tumor tissue, RGD peptide insertion significantly reduced transgene expression in all mutational backgrounds compared to untargeted vectors, just as they did in liver. Cell transduction, however, was only significantly lower when HSG interactions were ablated, supporting previous observations that peptide targeting is ineffective in HSG-ablated vectors.[10, 36] Systemic administration of singly mutated AdH+C− or AdH−C+ vectors with RGD peptide insertions also resulted in significantly reduced luciferase expression compared to untargeted AdH+C− or AdH−C+ in nearly all other tissues tested (data not shown). Administration of AdH+C−RGD resulted in a significant increase in the tumor/liver ratio of both luciferase expression (p=0.005) and cell transduction (p=0.001) compared to untargeted AdH+C− (data not shown), an effect primarily due to very low levels of luciferase expression and gene delivery in the liver for this RGD targeted, CAR ablated vector.

Discussion

Engineering adenoviral vectors using peptide targeting motifs to improve transduction and transgene expression in tumor cells has been evaluated over the last decade, but many questions remain about the overall utility of this strategy. Evidence from this investigation and others suggests that the effectiveness of this approach might be limited, particularly when used in combination with mutations designed to reduce native interactions. *In vitro* results from this study show that in most cell types, the incorporation of peptides in the HI loop of the adenoviral fiber knob only modestly improve targeting when these vectors are mutated to ablate CAR interactions, HSG interactions, or both. In fact, the use of targeting peptides occasionally had a detrimental effect on luciferase expression and/or cell transduction compared to mutated vectors with no peptide insertions. The incorporation of RGD, NGR, or ASL peptides in a wild-type AdH+C+ vector, however, consistently improved luciferase expression over untargeted AdH+C+ virus in all cell types, with the greatest improvement observed for viral infection of cells expressing low levels of CAR receptor.

We observed only small improvements in peptide targeting of adenovirus using HSG-ablated vectors that also lack intact CAR interactions. Interestingly, although similar or

reduced luciferase expression was observed for AdH−C+RGD compared to untargeted AdH −C+, viral binding and uptake of the RGD-targeted vector often increased, particularly in cells lacking high levels of CAR receptor. Increased viral binding was also observed for RGD targeting of AdH+C− vectors in MDA-MB-435s or HT1080 cells, despite the reduced luciferase expression observed. Although defects in cell transduction for our singly mutated HSG- or CAR- vectors was expected based on the importance of these interactions for cell binding and internalization, our *in vitro* results suggest that the incorporation of RGD peptide in the HI loop often fails to overcome these deficiencies, even when more viral particles appear to bind cells. Prior observations also showed no improvement in tumor cell transduction and transgene expression for RGD targeted H-C-adenovirus despite the enhanced cell binding seen for the RGD targeted vectors.[36] We observed that detrimental effects on luciferase expression due to the presence of RGD peptide in the AdH−C+ vector was much greater in CAR-positive HT1080 cells, and unlike the CAR-deficient MDA-MB-435 cells, also correlated with reduced cell-associated viral DNA. Several explanations for the reduced transduction of RGD-targeted virus due to the presence of RGD peptide in the HI loop are possible, such as interference with native CAR interactions, reduced particle stability, cross-interference with integrins which affects virus internalization or viral sequestration due to RGD-mediated interactions with other tissues or circulating factors. Peptides other than RGD may have similar effects due to interfering ligand:receptor interactions. As such, our results are in agreement with previous studies showing that peptides inserted into the HI loop were ineffective for retargeting adenovirus *in vitro* or *in vivo* when mutations in the fiber shaft were used simultaneously to ablate HSG-mediated interactions.[10, 36] The inability of peptide motifs to target these mutated vectors was proposed to be due to structural changes in the KKTK-mutated fiber shaft that affect fiber knob function.[32]

Previous data suggest that modifying the HI loop with the RGD peptide motif can reduce native CAR-dependent viral binding.[47, 48] The data herein showed that in cell lines expressing αvβ3 and/or αvβ5 integrins, substantial improvement in transgene expression for adenovirus incorporating RGD peptide in the HI loop occurred only in the cell lines expressing little or no CAR.[49] Consistent with previous studies,[29, 43, 50] *in vitro* data from this investigation also showed substantially lower infection of CAR-positive HT1080 cells using AdH−C+RGD compared to AdH−C+. In fact, similar luciferase expression profiles were observed for AdH−C−RGD and AdH−C+RGD in HT1080 cells, suggesting that the combination of HSG binding mutations and RGD peptide insertion could both be reducing native CAR interactions. The CAR+RGD soluble knob protein was still effective as a competitive inhibitor, however, so the lack of an intact HSG binding site seems to be the primary factor reducing the effectiveness of both RGD targeting and native CAR interactions. This supports previous suggestions that the HSG mutation could be affecting fiber shaft structure,[10] thereby preventing the proper function of both the RGD-integrin and CAR binding sites in the fiber knob.

Utilization of targeted adenoviral vectors *in vivo* produced results that vary widely from those expected based on *in vitro* studies. Despite small improvements in HT1080 cell infection for the addition of NGR or ASL peptides to doubly-mutated AdH−C− vectors *in*

vitro, these motifs showed no ability to enhance tumor targeting in our *in vivo* model. The RGD peptide also failed to improve AdH−C− targeting of HT1080 tumors in mice, and in fact resulted in lower luciferase expression and viral gene delivery compared to untargeted controls in all tissues tested. Prior results using an RGD-targeted adenoviral vector with intact native interactions in non-tumor bearing mice show increased transgene expression in all tissues tested, with the greatest increase observed in kidney.[51] Our results, however, showed decreased gene expression for AdH+C+RGD compared to AdH+C+ in all tissues except kidney, where we observed a small but insignificant increase in luciferase expression for the RGD targeted virus. The inability of RGD to improve targeting of wild-type adenovirus to the highly vascularized HT1080 tumors was perhaps not surprising given the small increases in luciferase expression and transduction seen for RGD targeted AdH+C+ in HT1080 cells *in vitro*. One factor could be that contributions from RGD-integrin binding with an affinity of 100 nM[21, 52] are quite weak in comparison to the much stronger 3–8 nM native CAR interaction with fiber knob used by Ad5 to bind cells.[42, 53] In fact, most peptides suffer from this limitation of relatively low binding affinity for their receptor that can only partially be compensated for by an increase in ligand number (36 per virion for HI loop insertions into fiber knob).

Very low levels of CAR expression have been observed in MDA-MB-435 cells,[31, 54, 55] and data from our lab also suggests only low levels of CAR in CHO K1 and ES-2 cells. *In vitro* data from this study show much greater improvements in relative transgene expression and cell transduction in these CAR-negative cell types compared to HT1080 cells using the RGD targeting strategy in otherwise wild-type H+C+ vectors. HT1080, however, is the neoplastic origin of our tumor model and cell line shown in our lab and others to be CAR-positive, and it is not surprising that adenoviral vectors capable of interacting with CAR are the most effective on these tumors. Despite the inability of RGD, NGR, or ASL peptides to significantly improve tumor targeting in the HT1080 tumor model, this strategy could still be an effective means of overcoming the reduced adenoviral infection normally seen in other tumor types expressing low CAR. Even so, we did not observe a significant increase in tumor specificity of the AdH+C+RGD vector in MDA-MB-435 tumors. It thus appears that further work needs to be done in CAR-negative tumor models to validate the utility of this approach, and results from this study suggest that the overall benefit afforded by targeting strategies using short RGD, NGR, or ASL peptides of relatively low affinity may be of limited value *in vivo*. These results also underscore the need to discover or develop targeting ligands with substantially higher affinity than those used in the current study if adenoviral retargeting of tumors using peptides is to become a more efficient process.

Supplementary Material

Refer to Web version on PubMed Central for supplementary material.

Acknowledgements

The authors wish to thank Julie Poirot and Jessica Mullens for technical help with recombinant virus construction and preparation. Angie Bookout provided advice on analysis and presentation of the integrin expression data. Paul Card helped prepare the manuscript for publication, and Steve Kliewer provided a critical reading. Glen Nemerow was kind enough to share the 633 cell line with us. Optical imaging was facilitated by the UT Southwestern Small

Animal Imaging Research Program funded by NCI U24 CA126608. This work was supported by a Texas Higher Education Coordinating Board Advanced Technology Program grant and by NIH R01 CA115935 to RDG.

References

1. Huard J, et al. The route of administration is a major determinant of the transduction efficiency of rat tissues by adenoviral recombinants. Gene Ther. 1995; 2(2):107–115. [PubMed: 7719927]
2. Li Q, et al. Assessment of recombinant adenoviral vectors for hepatic gene therapy. Hum Gene Ther. 1993; 4(4):403–409. [PubMed: 8399487]
3. van der Eb MM, et al. Severe hepatic dysfunction after adenovirus-mediated transfer of the herpes simplex virus thymidine kinase gene and ganciclovir administration. Gene Ther. 1998; 5(4):451–458. [PubMed: 9614568]
4. Herz J, Gerard RD. Adenovirus-mediated transfer of low density lipoprotein receptor gene acutely accelerates cholesterol clearance in normal mice. Proc Natl Acad Sci U S A. 1993; 90(7):2812–2816. [PubMed: 8464893]
5. Tomko RP, Xu R, Philipson L. HCAR and MCAR: the human and mouse cellular receptors for subgroup C adenoviruses and group B coxsackieviruses. Proc Natl Acad Sci U S A. 1997; 94(7): 3352–3356. [PubMed: 9096397]
6. Nemerow GR, et al. Insights into adenovirus host cell interactions from structural studies. Virology. 2009; 384(2):380–388. [PubMed: 19019405]
7. Martin K, et al. Simultaneous CAR− and alpha V integrin-binding ablation fails to reduce Ad5 liver tropism. Mol Ther. 2003; 8(3):485–494. [PubMed: 12946322]
8. Einfeld DA, et al. Reducing the native tropism of adenovirus vectors requires removal of both CAR and integrin interactions. J Virol. 2001; 75(23):11284–11291. [PubMed: 11689608]
9. Koizumi N, et al. Reduction of natural adenovirus tropism to mouse liver by fiber-shaft exchange in combination with both CAR− and alphav integrin-binding ablation. J Virol. 2003; 77(24):13062–13072. [PubMed: 14645563]
10. Bayo-Puxan N, et al. Role of the putative heparan sulfate glycosaminoglycan-binding site of the adenovirus type 5 fiber shaft on liver detargeting and knob-mediated retargeting. J Gen Virol. 2006; 87(Pt 9):2487–2495. [PubMed: 16894186]
11. Nicklin SA, et al. The influence of adenovirus fiber structure and function on vector development for gene therapy. Mol Ther. 2005; 12(3):384–393. [PubMed: 15993650]
12. Waddington SN, et al. Adenovirus serotype 5 hexon mediates liver gene transfer. Cell. 2008; 132(3):397–409. [PubMed: 18267072]
13. Kalyuzhniy O, et al. Adenovirus serotype 5 hexon is critical for virus infection of hepatocytes in vivo. Proc Natl Acad Sci U S A. 2008; 105(14):5483–5488. [PubMed: 18391209]
14. Vigant F, et al. Substitution of hexon hypervariable region 5 of adenovirus serotype 5 abrogates blood factor binding and limits gene transfer to liver. Mol Ther. 2008; 16(8):1474–1480. [PubMed: 18560416]
15. Dechecchi MC, et al. Heparan sulfate glycosaminoglycans are receptors sufficient to mediate the initial binding of adenovirus types 2 and 5. J Virol. 2001; 75(18):8772–8780. [PubMed: 11507222]
16. Dechecchi MC, et al. Heparan sulfate glycosaminoglycans are involved in adenovirus type 5 and 2-host cell interactions. Virology. 2000; 268(2):382–390. [PubMed: 10704346]
17. Smith TA, et al. Receptor interactions involved in adenoviral-mediated gene delivery after systemic administration in non-human primates. Hum Gene Ther. 2003; 14(17):1595–1604. [PubMed: 14633402]
18. Smith TA, et al. Adenovirus serotype 5 fiber shaft influences in vivo gene transfer in mice. Hum Gene Ther. 2003; 14(8):777–787. [PubMed: 12804140]
19. Hogg RT, Thorpe P, Gerard RD. Retargeting adenoviral vectors to improve gene transfer into tumors. Cancer Gene Ther. 2011; 18:275–287. [PubMed: 21183946]
20. Ruoslahti E. Targeting tumor vasculature with homing peptides from phage display. Semin Cancer Biol. 2000; 10(6):435–442. [PubMed: 11170865]

21. Koivunen E, Wang B, Ruoslahti E. Phage libraries displaying cyclic peptides with different ring sizes: ligand specificities of the RGD-directed integrins. Biotechnology (N Y). 1995; 13(3):265–270. [PubMed: 9634769]
22. Pasqualini R, Koivunen E, Ruoslahti E. Alpha v integrins as receptors for tumor targeting by circulating ligands. Nat Biotechnol. 1997; 15(6):542–546. [PubMed: 9181576]
23. Curnis F, et al. Differential binding of drugs containing the NGR motif to CD13 isoforms in tumor vessels, epithelia, and myeloid cells. Cancer Res. 2002; 62(3):867–874. [PubMed: 11830545]
24. Pasqualini R, et al. Aminopeptidase N is a receptor for tumor-homing peptides and a target for inhibiting angiogenesis. Cancer Res. 2000; 60(3):722–727. [PubMed: 10676659]
25. Arap W, Pasqualini R, Ruoslahti E. Cancer treatment by targeted drug delivery to tumor vasculature in a mouse model. Science. 1998; 279(5349):377–380. [PubMed: 9430587]
26. Garde SV, et al. Binding and internalization of NGR-peptide-targeted liposomal doxorubicin (TVT-DOX) in CD13-expressing cells and its antitumor effects. Anticancer Drugs. 2007; 18(10): 1189–1200. [PubMed: 17893520]
27. Pastorino F, et al. Vascular damage and anti-angiogenic effects of tumor vessel-targeted liposomal chemotherapy. Cancer Res. 2003; 63(21):7400–7409. [PubMed: 14612539]
28. Pastorino F, et al. Targeting liposomal chemotherapy via both tumor cell-specific and tumor vasculature-specific ligands potentiates therapeutic efficacy. Cancer Res. 2006; 66(20):10073–10082. [PubMed: 17047071]
29. Mizuguchi H, et al. A simplified system for constructing recombinant adenoviral vectors containing heterologous peptides in the HI loop of their fiber knob. Gene Ther. 2001; 8(9):730–735. [PubMed: 11406768]
30. Majhen D, et al. Disulfide bond formation in NGR fiber-modified adenovirus is essential for retargeting to aminopeptidase N. Biochem Biophys Res Commun. 2006; 348(1):278–287. [PubMed: 16876116]
31. Jullienne B, et al. Efficient delivery of angiostatin K1-5 into tumors following insertion of an NGR peptide into adenovirus capsid. Gene Ther. 2009; 16(12):1405–1415. [PubMed: 19641530]
32. Bayo-Puxan N, et al. Replacement of adenovirus type 5 fiber shaft heparan sulfate proteoglycan-binding domain with RGD for improved tumor infectivity and targeting. Hum Gene Ther. 2009; 20(10):1214–1221. [PubMed: 19537946]
33. Rein DT, et al. Gene transfer to cervical cancer with fiber-modified adenoviruses. Int J Cancer. 2004; 111(5):698–704. [PubMed: 15252838]
34. Li P, et al. Use of adenoviral vectors to target chemotherapy to tumor vascular endothelial cells suppresses growth of breast cancer and melanoma. Mol Ther. 2010; 18(5):921–928. [PubMed: 20179680]
35. Singh R, Kostarelos K. Designer adenoviruses for nanomedicine and nanodiagnostics. Trends Biotechnol. 2009; 27(4):220–229. [PubMed: 19251331]
36. Kritz AB, et al. Adenovirus 5 fibers mutated at the putative HSPG-binding site show restricted retargeting with targeting peptides in the HI loop. Mol Ther. 2007; 15(4):741–749. [PubMed: 17245351]
37. Roelvink PW, et al. Identification of a conserved receptor-binding site on the fiber proteins of CAR-recognizing adenoviridae. Science. 1999; 286(5444):1568–1571. [PubMed: 10567265]
38. Chartier C, et al. Efficient generation of recombinant adenovirus vectors by homologous recombination in Escherichia coli. J Virol. 1996; 70(7):4805–4810. [PubMed: 8676512]
39. Gerard, RD.; Meidell, RS. Adenovirus vectors, in DNA Cloning: A Practical Approach. Hames, BD.; Glover, D., editors. Oxford: Oxford University Press; 1995. p. 285-307.
40. Von Seggern DJ, et al. Adenovirus vector pseudotyping in fiber-expressing cell lines: improved transduction of Epstein-Barr virus-transformed B cells. J Virol. 2000; 74(1):354–362. [PubMed: 10590124]
41. Hogg RT, Garcia JA, Gerard RD. Adenoviral targeting of gene expression to tumors. Cancer Gene Ther. 2010; 17:375–386. [PubMed: 20139924]
42. Henry LJ, et al. Characterization of the knob domain of the adenovirus type 5 fiber protein expressed in Escherichia coli. J Virol. 1994; 68(8):5239–5246. [PubMed: 8035520]

43. Sharma A, et al. Adenovirus receptors and their implications in gene delivery. Virus Res. 2009; 143(2):184–194. [PubMed: 19647886]
44. Xia D, et al. Crystal structure of the receptor-binding domain of adenovirus type 5 fiber protein at 1.7 A resolution. Structure. 1994; 2(12):1259–1270. [PubMed: 7704534]
45. Pandha HS, et al. Coxsackie B and adenovirus receptor, integrin and major histocompatibility complex class I expression in human prostate cancer cell lines: implications for gene therapy strategies. Prostate Cancer Prostatic Dis. 2003; 6(1):6–11. [PubMed: 12664058]
46. Wu Z, et al. microPET of tumor integrin alphavbeta3 expression using 18F-labeled PEGylated tetrameric RGD peptide (18F-FPRGD4). J Nucl Med. 2007; 48(9):1536–1544. [PubMed: 17704249]
47. Wu H, et al. Double modification of adenovirus fiber with RGD and polylysine motifs improves coxsackievirus-adenovirus receptor-independent gene transfer efficiency. Hum Gene Ther. 2002; 13(13):1647–1653. [PubMed: 12228019]
48. Bilbao R, et al. Fetal muscle gene transfer is not enhanced by an RGD capsid modification to high-capacity adenoviral vectors. Gene Ther. 2003; 10(21):1821–1829. [PubMed: 12960972]
49. Koizumi N, et al. Generation of fiber-modified adenovirus vectors containing heterologous peptides in both the HI loop and C terminus of the fiber knob. J Gene Med. 2003; 5(4):267–276. [PubMed: 12692861]
50. Hidaka C, et al. CAR-dependent and CAR-independent pathways of adenovirus vector-mediated gene transfer and expression in human fibroblasts. J Clin Invest. 1999; 103(4):579–587. [PubMed: 10021467]
51. Reynolds P, Dmitriev I, Curiel D. Insertion of an RGD motif into the HI loop of adenovirus fiber protein alters the distribution of transgene expression of the systemically administered vector. Gene Ther. 1999; 6(7):1336–1339. [PubMed: 10455445]
52. Assa-Munt N, et al. Solution structures and integrin binding activities of an RGD peptide with two isomers. Biochemistry. 2001; 40(8):2373–2378. [PubMed: 11327857]
53. Kirby I, et al. Adenovirus type 9 fiber knob binds to the coxsackie B virus-adenovirus receptor (CAR) with lower affinity than fiber knobs of other CAR-binding adenovirus serotypes. J Virol. 2001; 75(15):7210–7214. [PubMed: 11435605]
54. Niu G, et al. In vivo bioluminescence tumor imaging of RGD peptide-modified adenoviral vector encoding firefly luciferase reporter gene. Mol Imaging Biol. 2007; 9(3):126–134. [PubMed: 17297551]
55. Xiong Z, et al. Imaging chemically modified adenovirus for targeting tumors expressing integrin alphavbeta3 in living mice with mutant herpes simplex virus type 1 thymidine kinase PET reporter gene. J Nucl Med. 2006; 47(1):130–139. [PubMed: 16391197]
56. Minea RO, et al. Vicrostatin - an anti-invasive multi-integrin targeting chimeric disintegrin with tumor anti-angiogenic and pro-apoptotic activities. PLoS One. 2010; 5(6):e10929. [PubMed: 20532165]
57. Demaegdt H, et al. Angiotensin AT4 receptor ligand interaction with cystinyl aminopeptidase and aminopeptidase N: [125I]Angiotensin IV only binds to the cystinyl aminopeptidase apo-enzyme. Eur J Pharmacol. 2006; 546(1–3):19–27. [PubMed: 16919623]
58. Garrigues HJ, et al. Integrin alphaVbeta3 Binds to the RGD motif of glycoprotein B of Kaposi's sarcoma-associated herpesvirus and functions as an RGD-dependent entry receptor. J Virol. 2008; 82(3):1570–1580. [PubMed: 18045938]
59. Shim JS, et al. Irreversible inhibition of CD13/aminopeptidase N by the antiangiogenic agent curcumin. Chem Biol. 2003; 10(8):695–704. [PubMed: 12954328]
60. Terauchi M, et al. Inhibition of APN/CD13 leads to suppressed progressive potential in ovarian carcinoma cells. BMC Cancer. 2007; 7:140. [PubMed: 17655775]
61. Freedland SJ, et al. Loss of CD10 (neutral endopeptidase) is a frequent and early event in human prostate cancer. Prostate. 2003; 55(1):71–80. [PubMed: 12640663]
62. Liu AY. Differential expression of cell surface molecules in prostate cancer cells. Cancer Res. 2000; 60(13):3429–3434. [PubMed: 10910052]

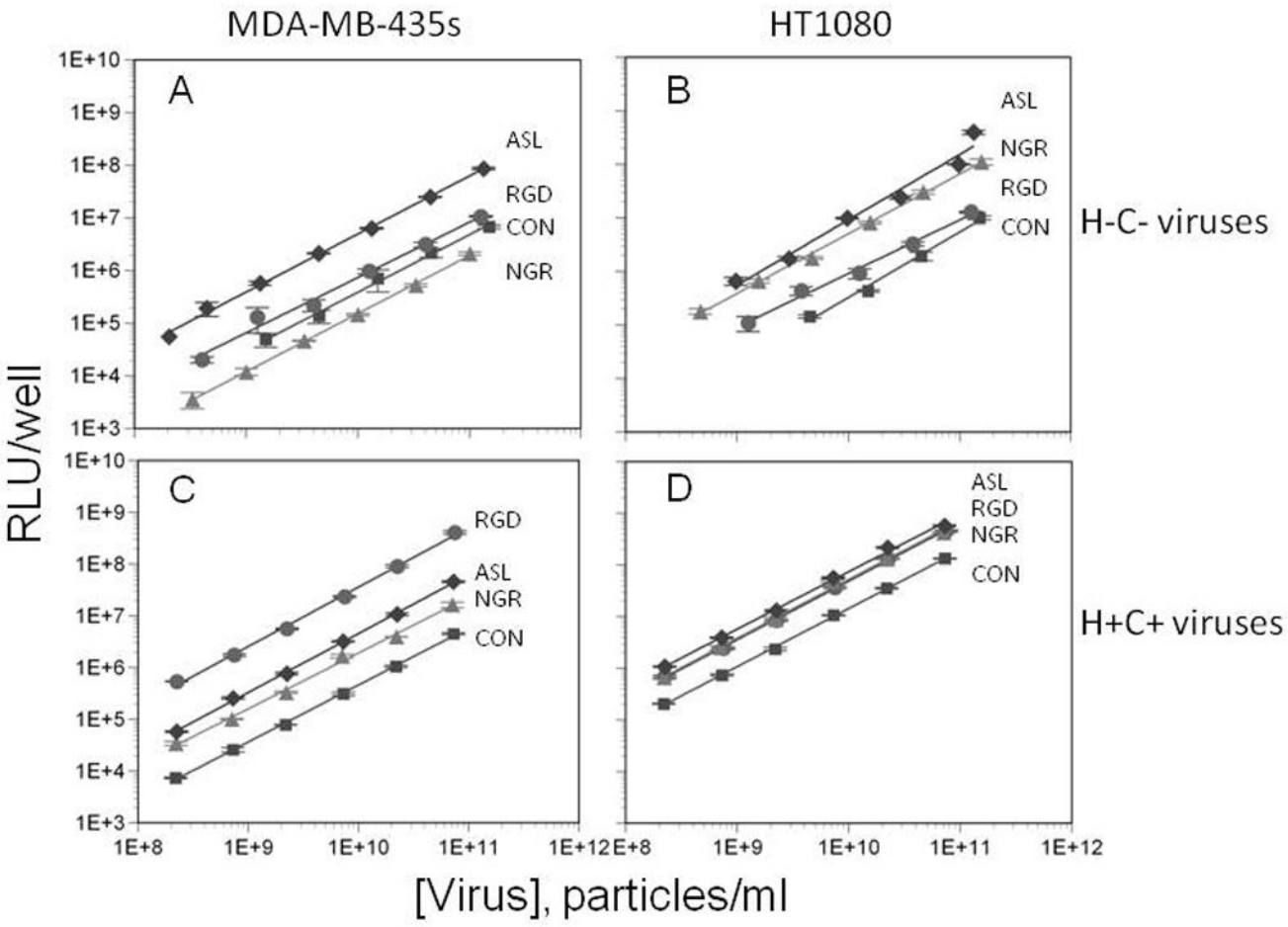

Figure 1. Effect of targeting peptides on viral infection of tumor cells in vitro

Tumor cells expressing undetectable levels of CAR (MDA-MB-435s) or high levels of CAR (HT1080) were infected with varying concentrations of adenoviral particles either with or without targeting peptide sequences (CON, squares) inserted into the HI loop of the fiber knob. Targeting peptide sequences included RGD (circles), NGR (triangles), or ASL (diamonds) moieties. Both vector detargeted for native interactions (AdH−C−, panels A and B) or wild-type vector (AdH+C+, panels C and D) were used as platforms to evaluate the effects of peptide targeting on cell infection and luciferase expression in the two tumor cell types. Error bars indicate standard deviation of mean values for wells infected in triplicate. Data for each virus were fitted to a power function, and the equations used to calculate the luciferase data in Tables II and III.

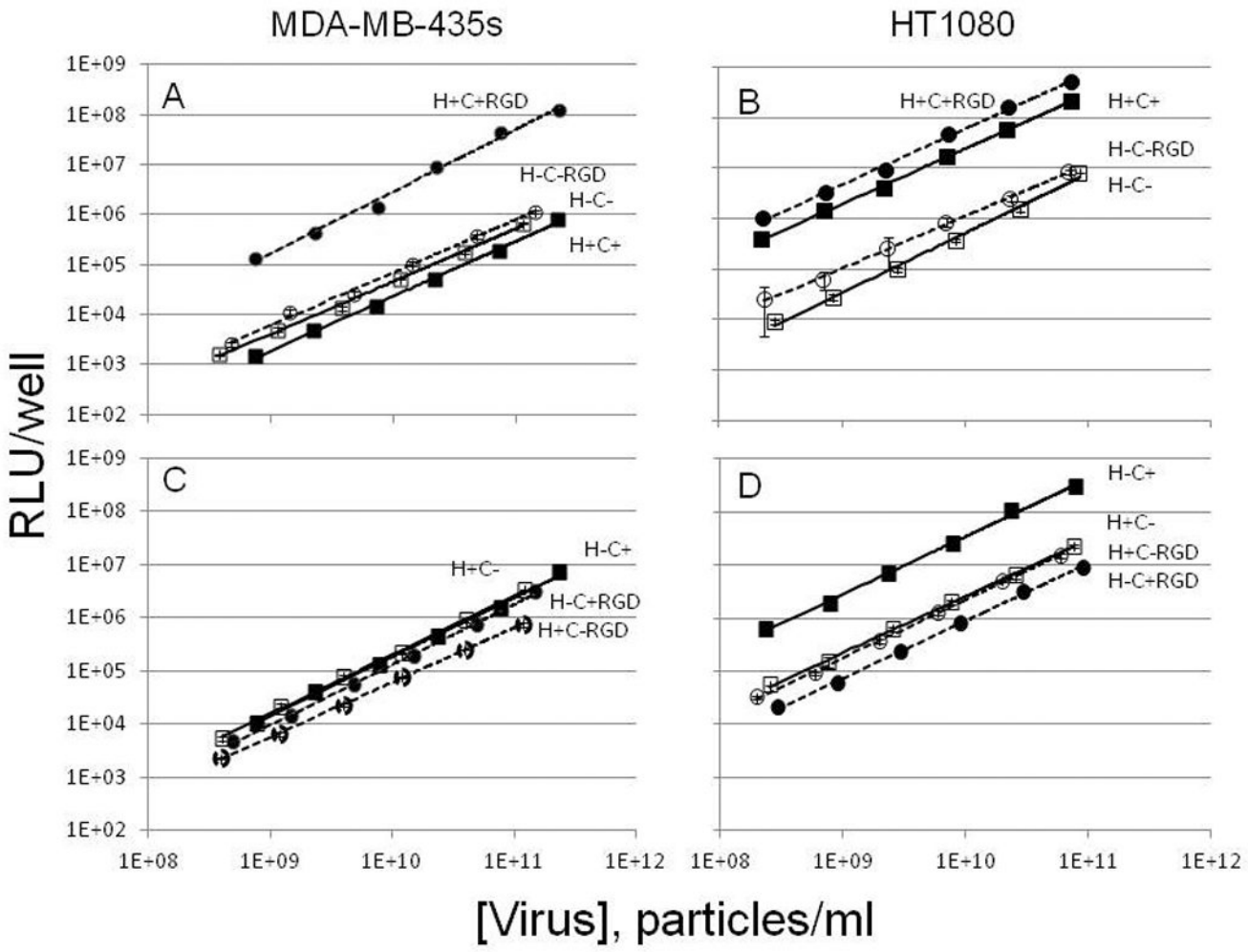

Figure 2. Effect of RGD peptide on retargeting of adenoviral vectors harboring various combinations of mutations

Contribution of RGD peptide to targeting of doubly mutated AdH−C− (open symbols) or wild type AdH+C+ (closed symbols) vectors in MDA-MB-435 (panel A) or HT1080 (panel B) tumor cells. Effect of RGD targeting in MDA-MB-435 (panel C) or HT1080 (panel D) cells for singly mutated vectors designed to ablate either CAR (AdH+C−, open symbols) or HSG (AdH−C+, closed symbols) interactions with adenoviral ligands. Vectors without RGD are indicated by solid lines and square symbols, while vectors with the RGD peptide are shown as dotted lines and circular symbols. Error bars indicate standard deviation of mean values for wells infected in triplicate. Data for each virus were fitted to a power function, and the equations used to calculate the luciferase data in Table IV.

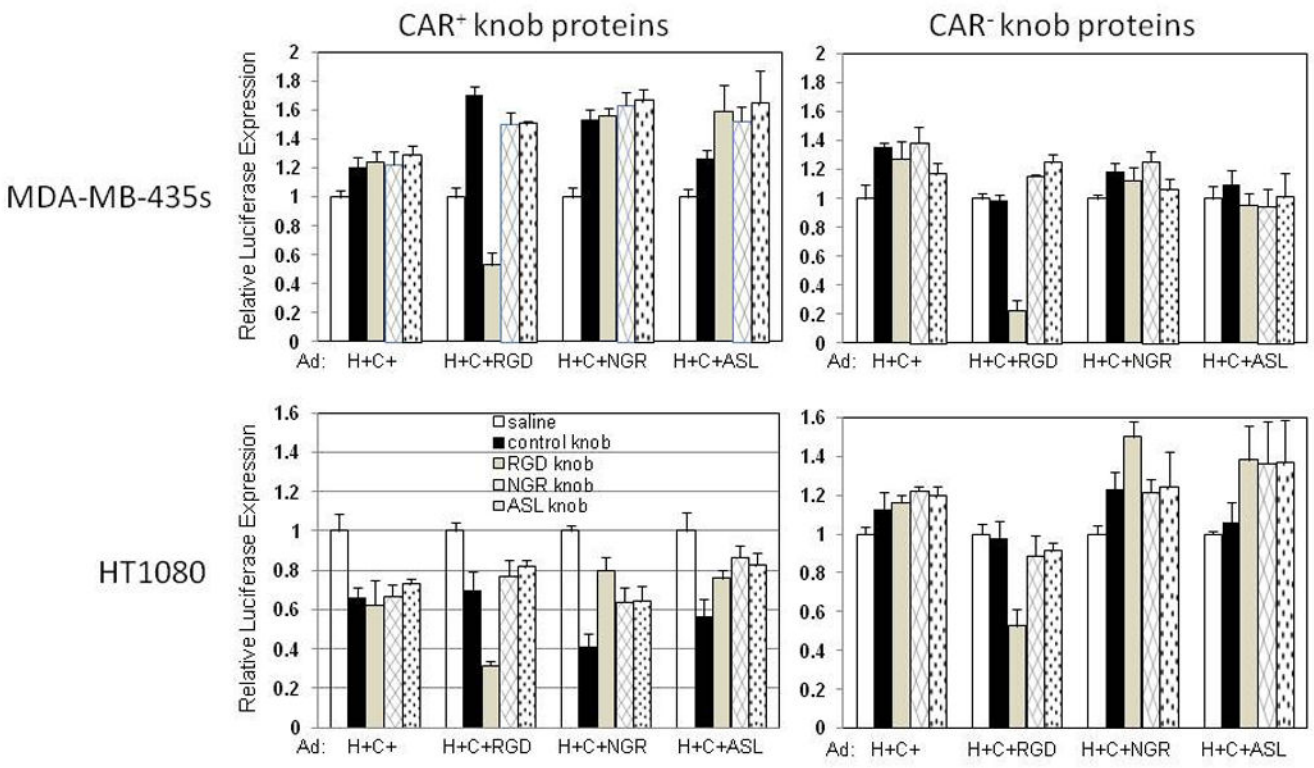

Figure 3. Inhibition of targeted virus infectivity using soluble knob proteins as competitors

MDA-MB-435S and HT1080 cells were preincubated with soluble peptide knob proteins (either CAR-positive or CAR-negative) to bind receptors and eclipse viral infection, and then infected with either AdH+C+ or a peptide targeted virus as indicated. Luciferase expression was normalized to that present in the absence of any added knob (open bars) for the individual viruses. No peptide (black bars), RGD peptide (gray bars), NGR peptide (hatched bars) and ASL peptide (stippled bars). Error bars indicate standard deviation of mean values for wells infected in triplicate.

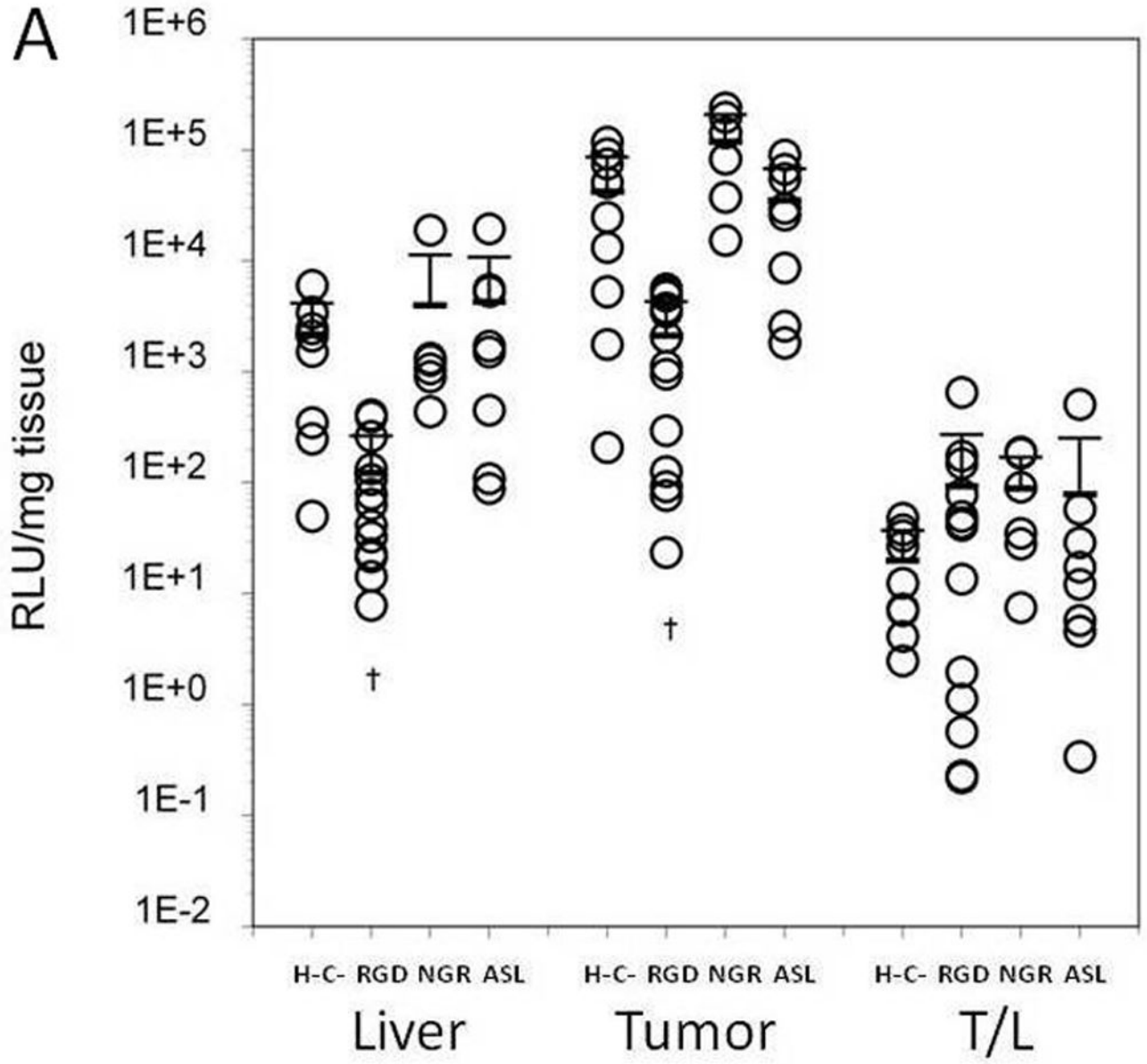

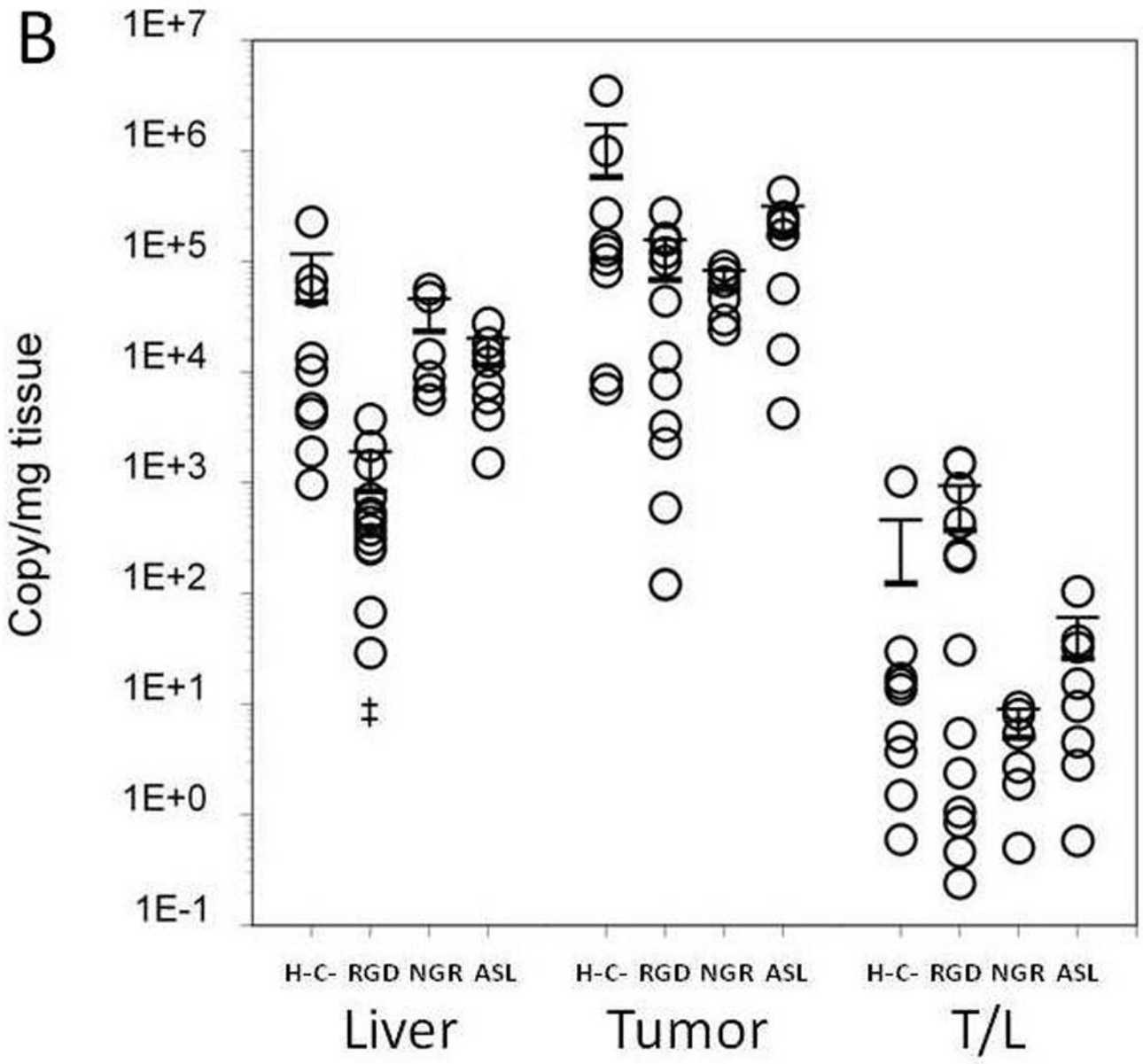

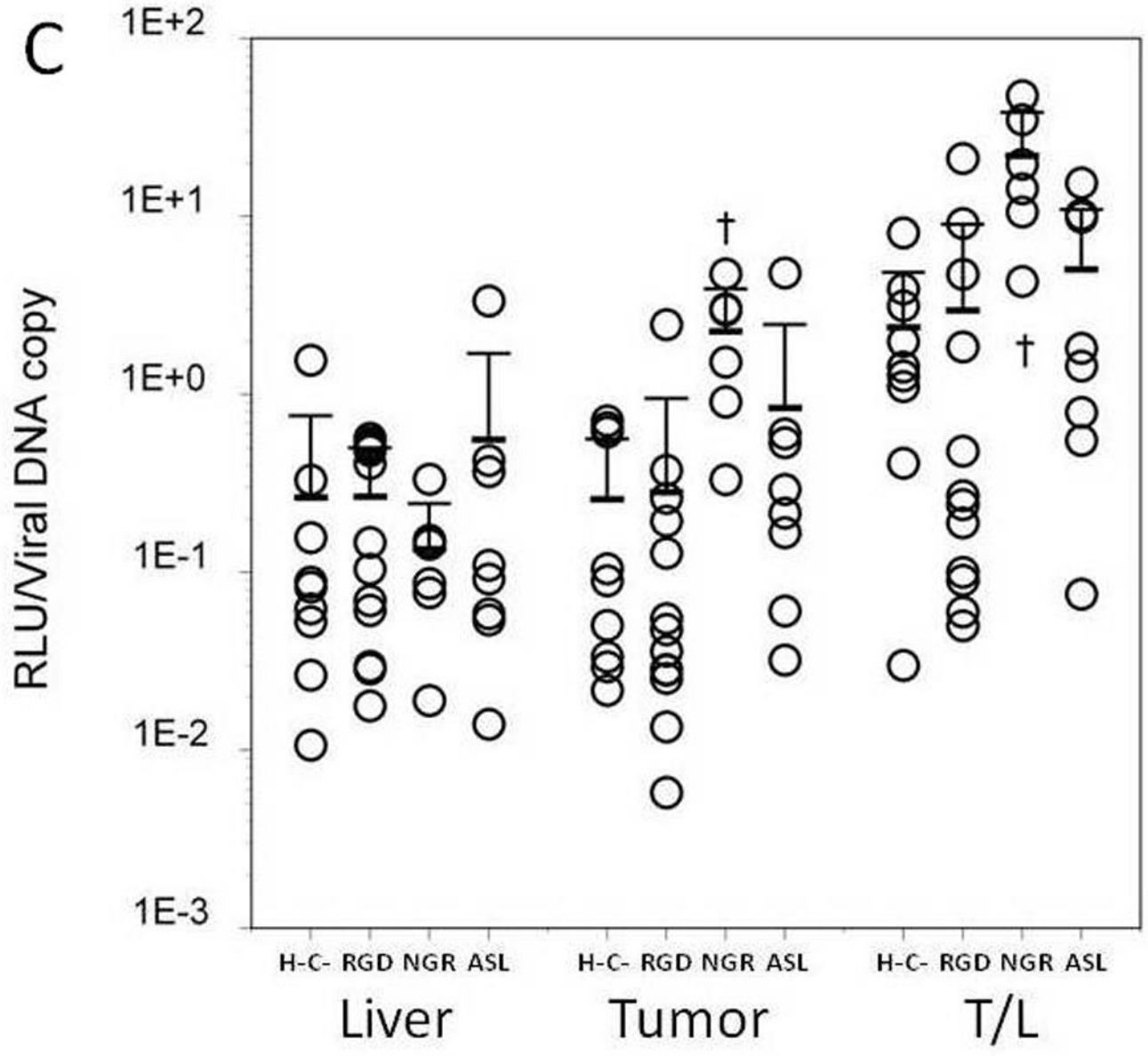

Figure 4. Effect of targeting peptides incorporated into fiber knob of AdH−C− vectors on biodistribution in HT1080 tumor bearing mice

Adenoviral vectors detargeted for CAR and HSG interactions with or without RGD, NGR, or ASL targeting peptides were intravenously administered at a dose of 10^{11} particles per mouse. Values for individual mice are shown, with mean and standard deviation represented by horizontal and error bars. Significant differences between experimental groups and the control are indicated by daggers († $p<0.01$) and double daggers (‡ $p\leq0.001$). Panel A, luciferase expression was quantified in tumor and liver using biochemical means and is expressed in RLU per milligram of tissue. T/L, tumor liver ratio as an indicator of tumor targeting was calculated for each animal. Panel B, effect of peptide insertions into fiber knob on biodistribution of viral DNA was quantified using real-time PCR. Gene delivery

expressed as viral DNA copies per mg of tissue was measured in liver and tumor. Panel C, specific activity, measured in RLU per DNA copy, was calculated from data for individual mice shown in the previous two panels.

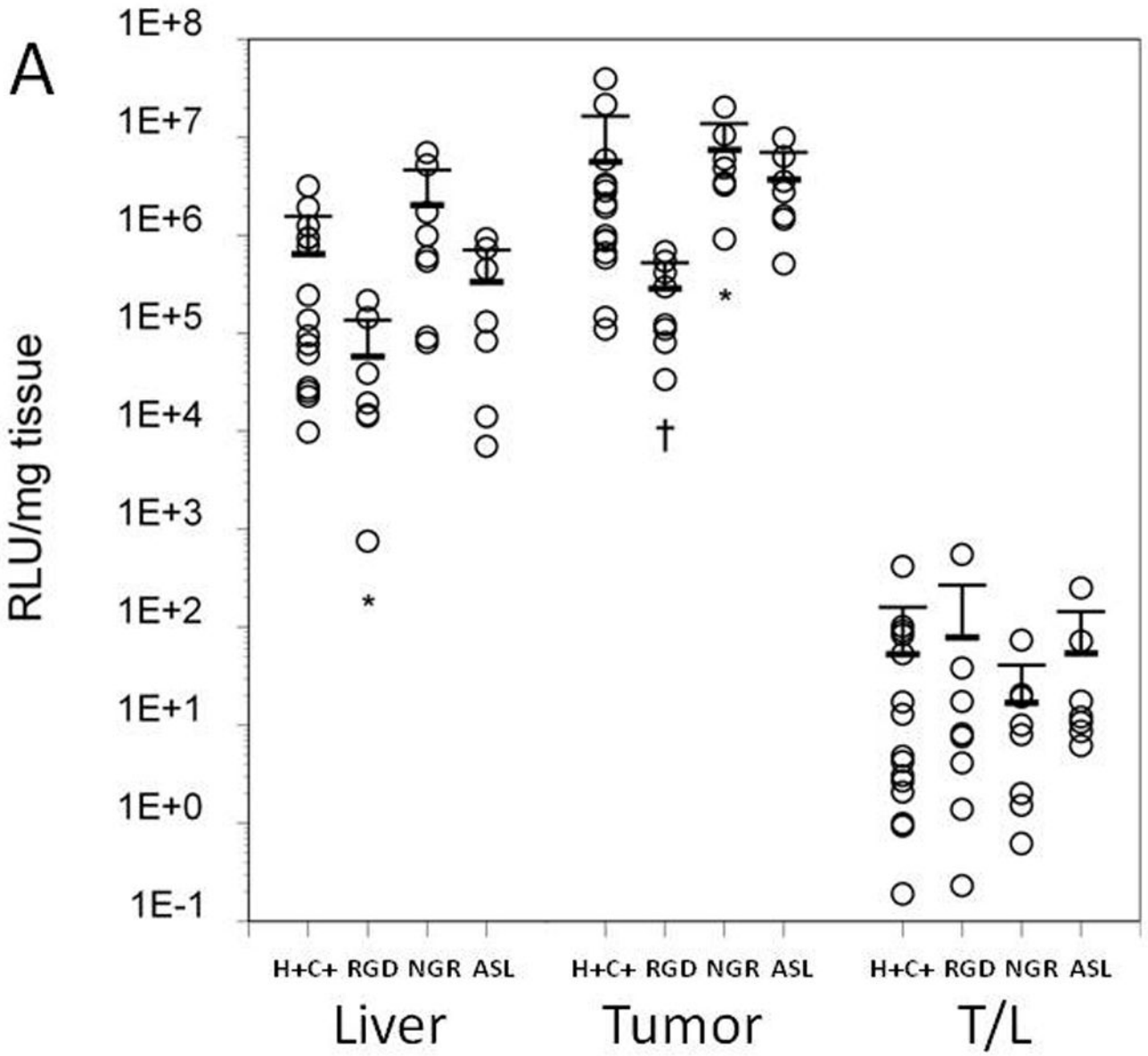

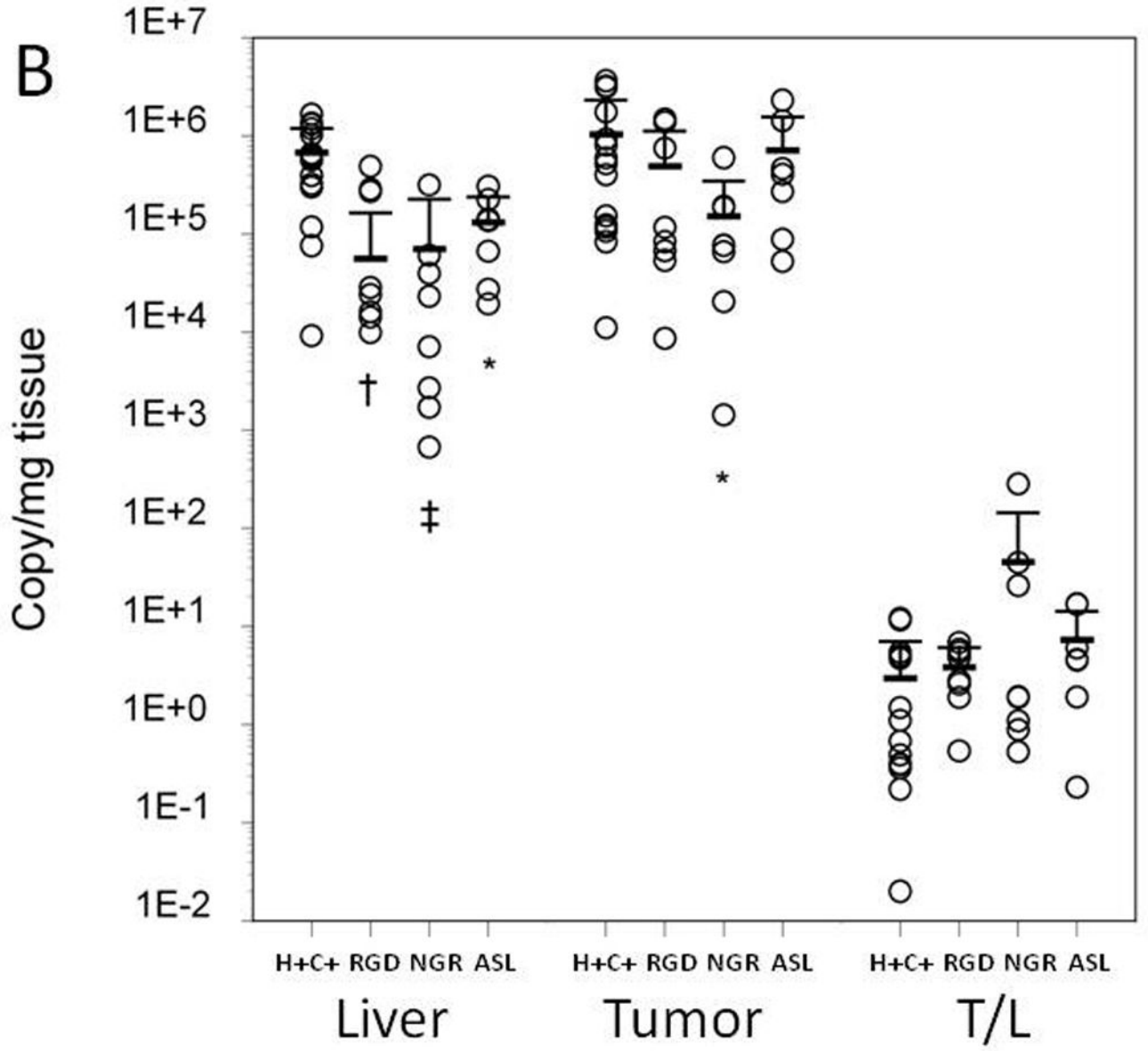

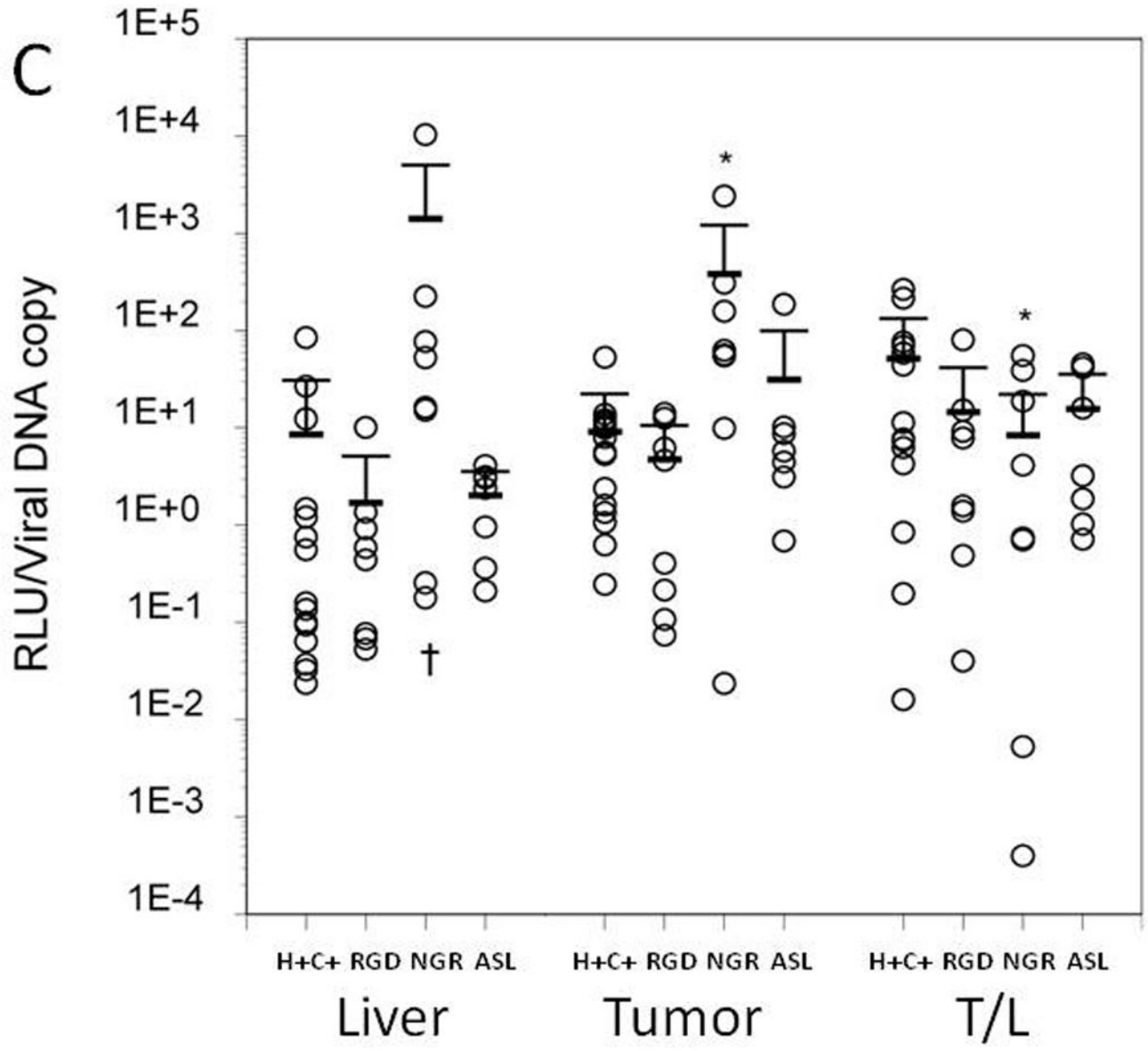

Figure 5. Effect of targeting peptides incorporated into AdH+C+ on biodistribution in HT1080 tumor bearing mice

Wild-type adenoviral vectors with or without RGD, NGR, or ASL targeting peptides were intravenously administered at a dose of 10^{11} particles per mouse. Values for individual mice are shown as circles, with mean and standard deviation represented by horizontal and error bars. Significant differences between experimental and control groups are indicated by asterisks (* $p<0.05$), daggers († $p<0.01$) and double daggers (‡ $p\leq0.001$). Panel A, Luciferase expression was quantified in tumor and liver using biochemical means and is expressed in RLU per milligram of tissue. T/L, tumor liver ratio as an indicator of tumor targeting was calculated for each animal. Panel B, effect of targeting peptides on biodistribution of viral DNA. Gene delivery in viral DNA copy per mg of tissue was measured in liver and tumor using real-time PCR. Panel C, specific activity, measured in

RLU per DNA copy, was calculated from data for individual mice shown in the previous two panels.

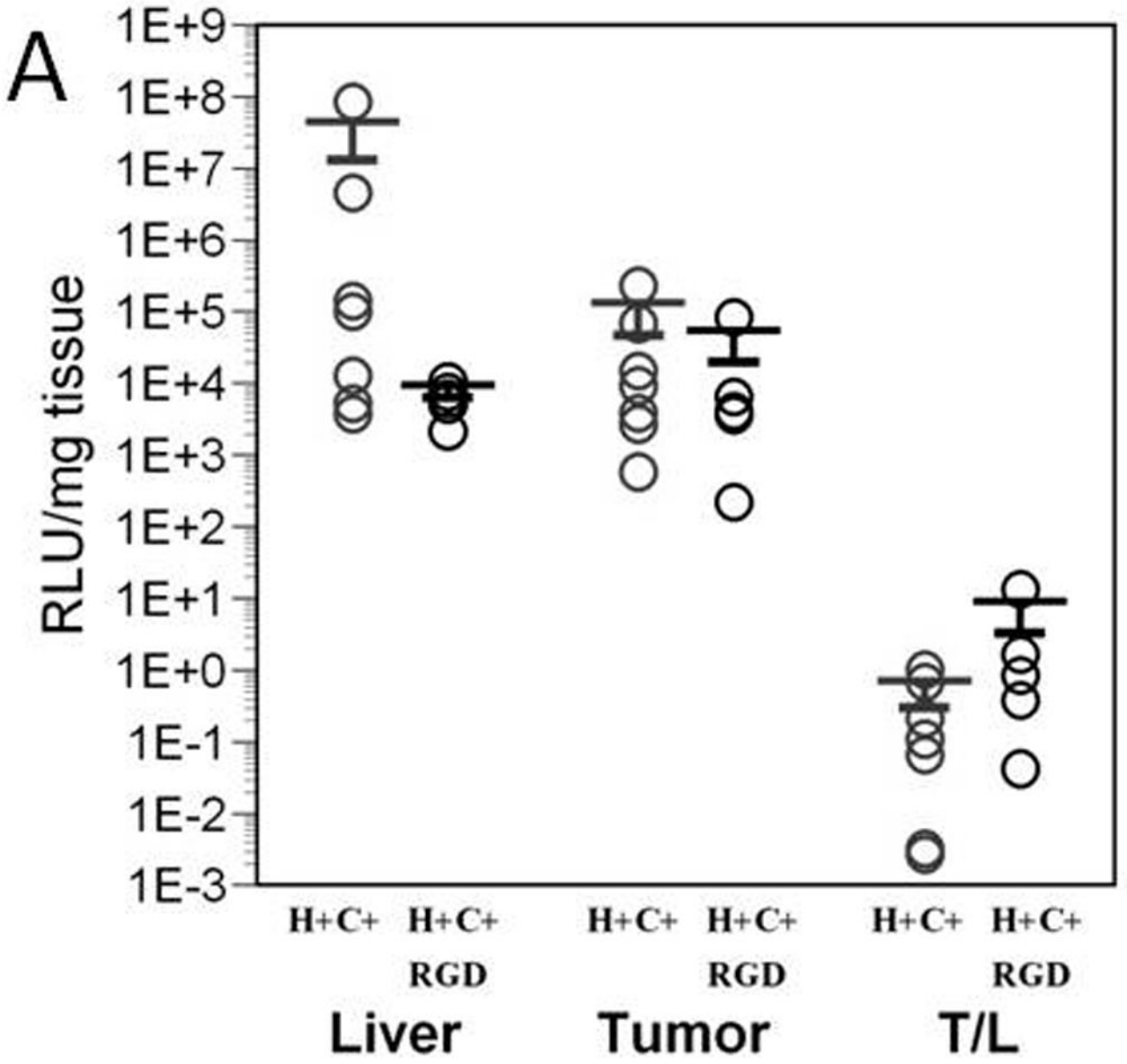

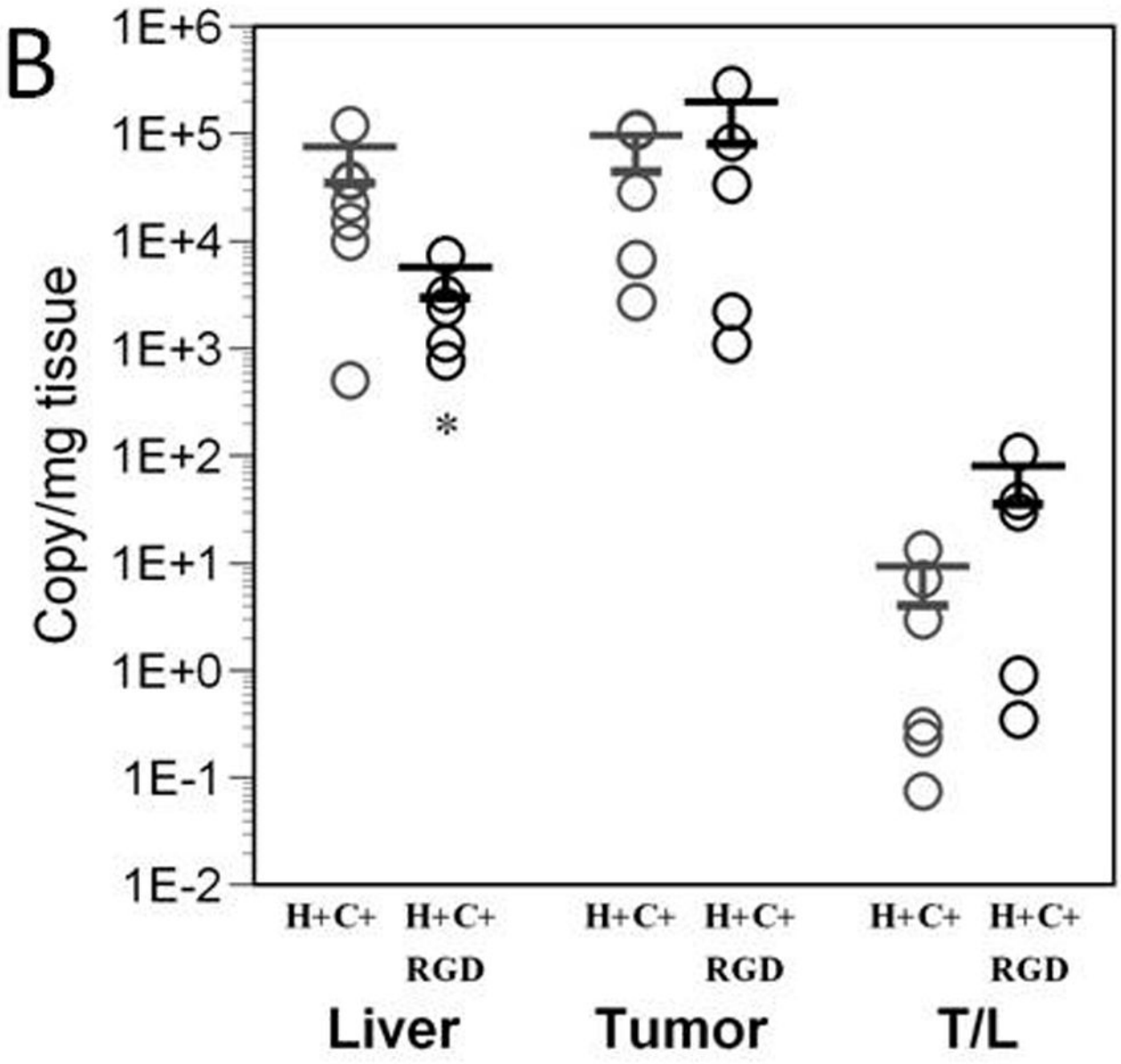

Figure 6. Effect of the RGD targeting peptide on adenoviral targeting in mice harboring MDA-MB-435s tumors

Wild-type adenoviral vectors either with (H+C+RGD) or without (H+C+) RGD peptide inserted into the fiber knob domain were intravenously administered at a dose of 10^{11} particles per mouse. Values for individual mice are shown, with mean and standard deviation represented by horizontal and error bars. Significant differences between experimental and control groups are indicated by asterisks (* $p<0.05$). Panel A, luciferase expression was quantified in tumor and liver using biochemical means and is expressed in RLU per milligram of tissue. Panel B, effect of the RGD targeting peptide on biodistribution of adenoviral DNA. Gene delivery in viral DNA copy per mg of tissue was measured in liver and tumor using real-time PCR.

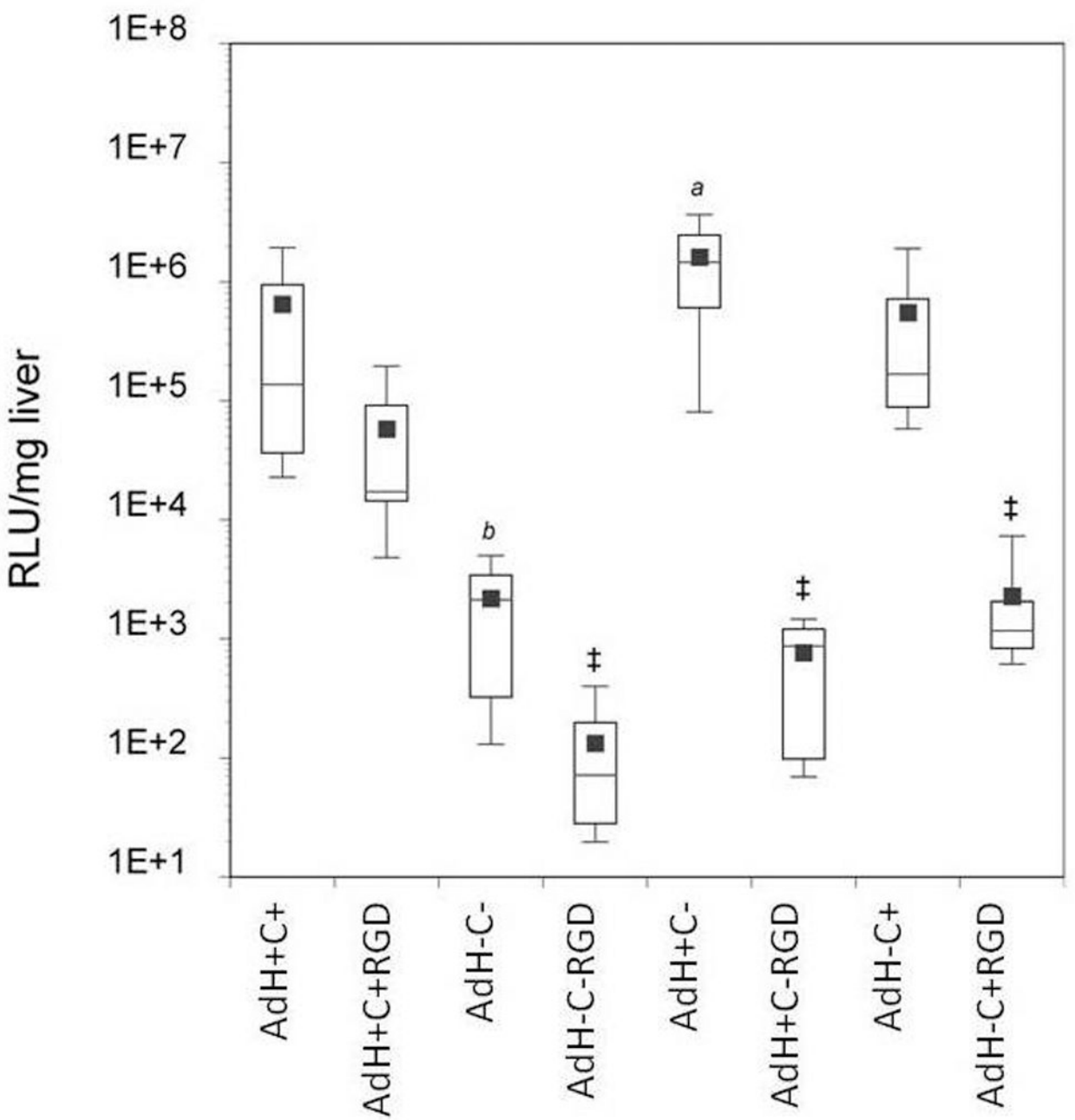

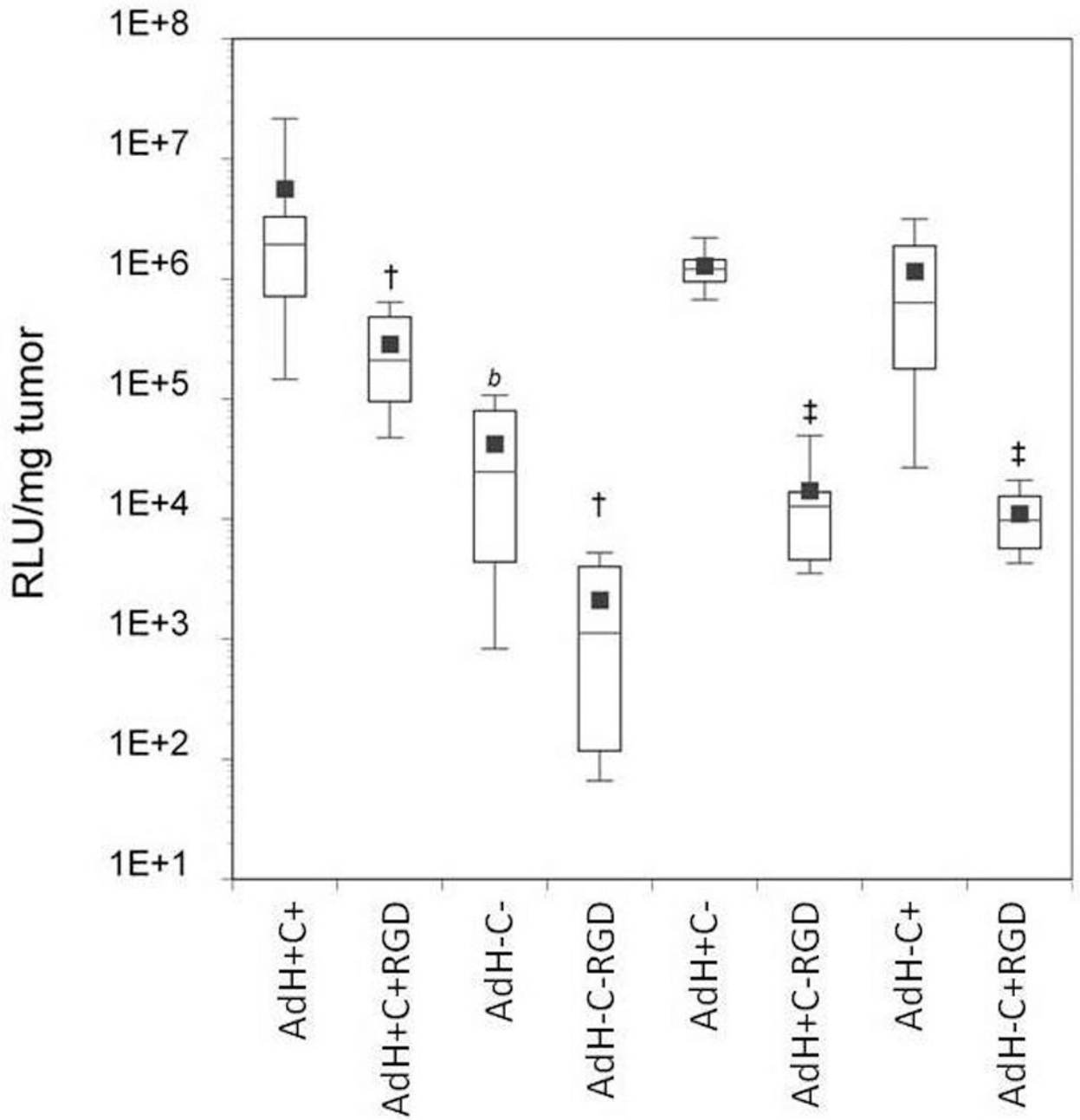

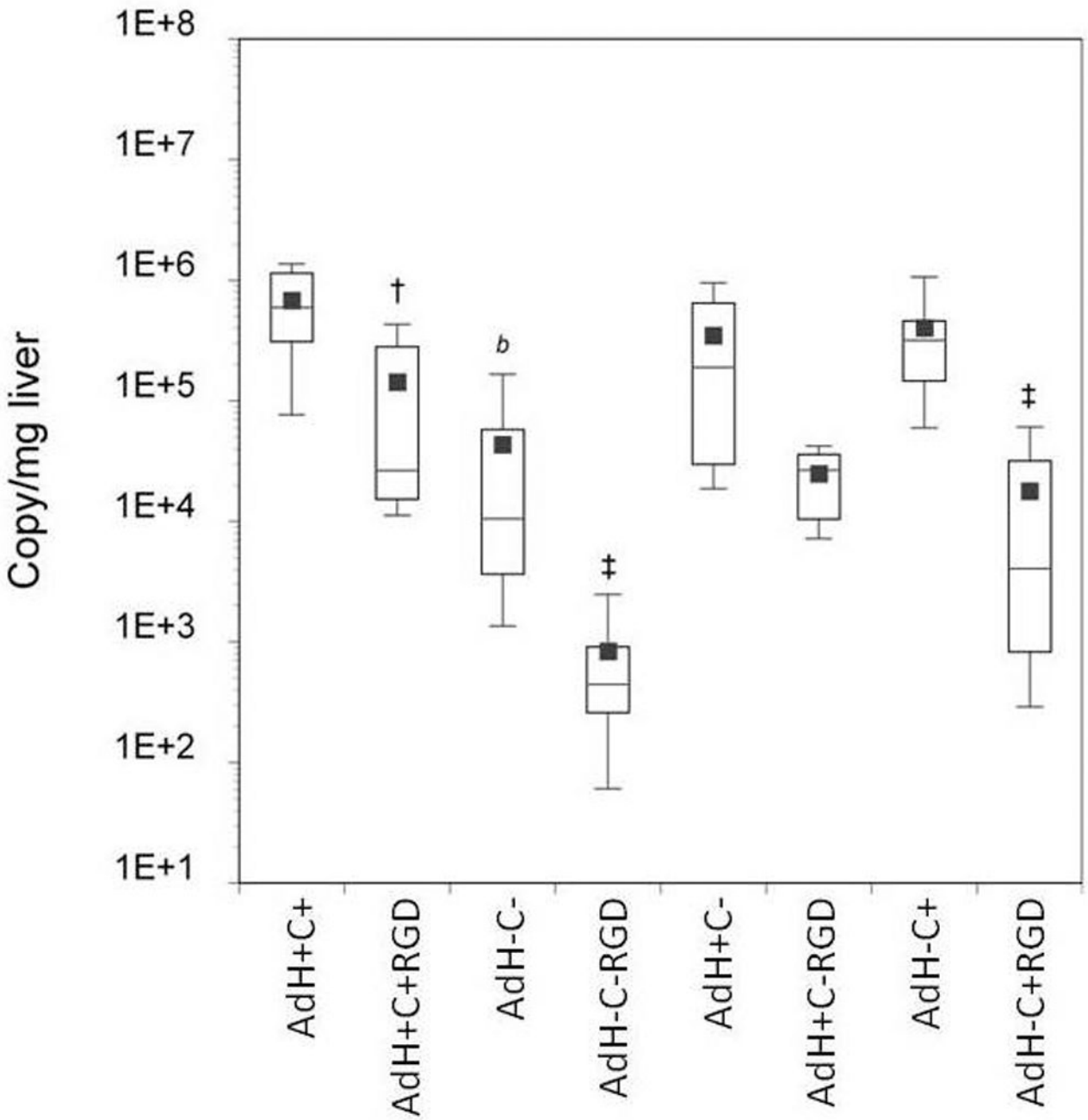

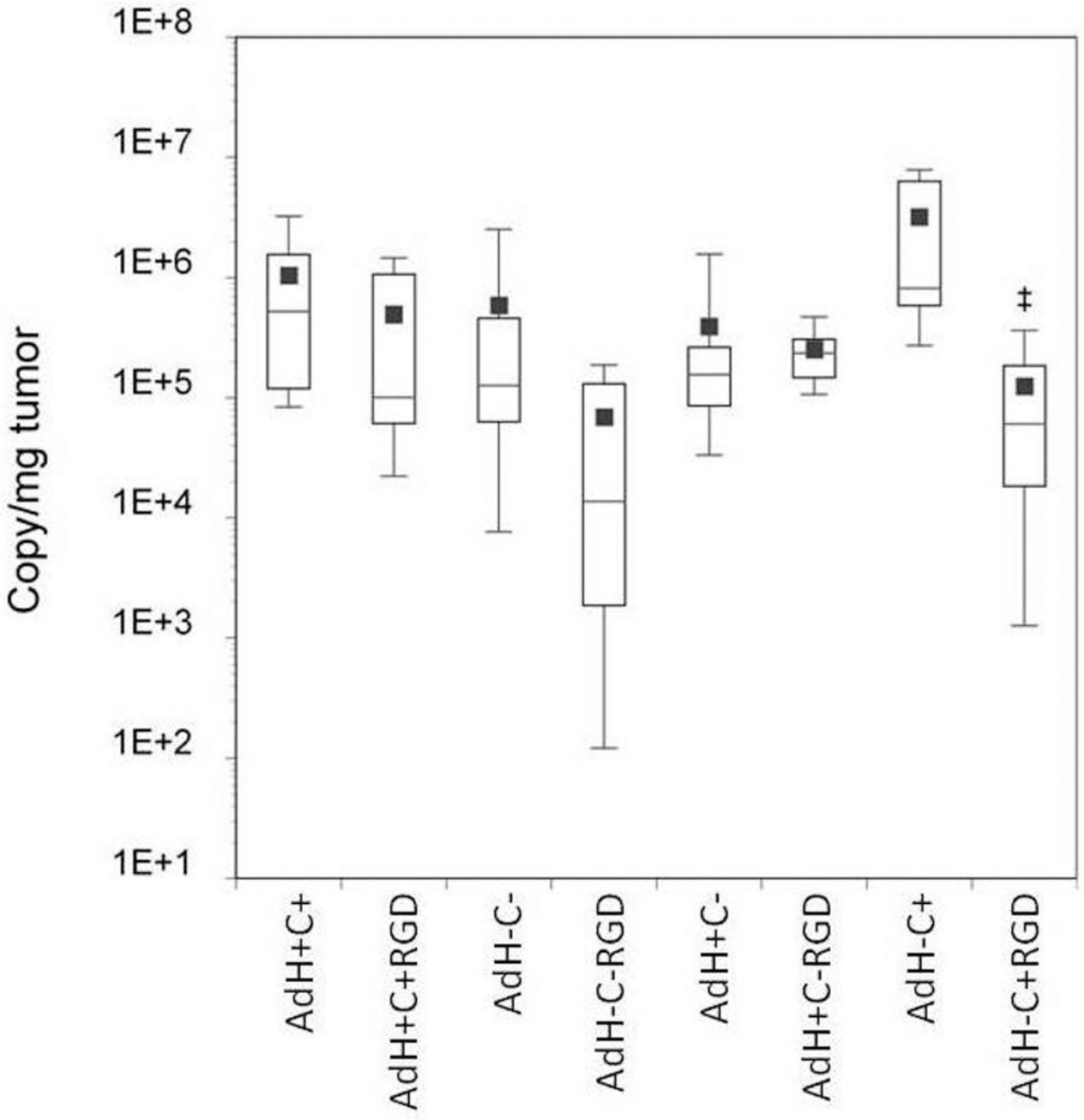

Figure 7. Comparison summary of wild-type, HSG- and/or CAR- mutated adenoviral vectors with and without RGD peptide insertions in HT1080 tumor bearing mice

Luciferase expression is expressed as RLU per mg of tissue for tumor and liver and viral transduction (viral DNA copies/mg) was assessed by real-time PCR. In the box plot, mean values are shown as solid blue boxes and median values by horizontal lines. 75% confidence intervals are shown as boxes and 95% confidence intervals are shown by double-sided error bars. Significant differences between experimental RGD targeted vectors compared to non-peptide controls are indicated by asterisks (* $p<0.05$), daggers († $p<0.01$) and double daggers (‡ $p\leq0.001$), and significant differences between mutated vectors without peptide

insertions as compared to wild-type vector (AdH+C+) are indicated by italicized letters (*a*, $p<0.05$ and *b*, $p\leq0.001$).

Table I

Expression levels of various receptors used for targeting adenoviruses by tumor cell lines.

Cell Line	Integrin expression[1]	CAR expression	APN/CD13[2] expression
MDA-MB-435S	Medium high ([31, 54–56] and Supplemental Figure 1)	Not detectable [19, 31, 54, 55]	Low [31]
CHOK1	High (Supplemental Figure 1)	Not detectable (our unpublished data and Supplemental Figure 3)	Low [57]
HT1080	Medium ([58] and Supplemental Figure 1)	High ([19] and our unpublished data)	Medium-high [26, 59]
ES-2	Medium (supplemental Figure 1)	Very low (our unpublished data)	High[60]
DU145	Medium low[45, 46]	Very high ([45]and our unpublished data)	Not detectable-low[61, 62]

[1] NGR peptide can use integrins as alternative mode of cell entry[31]

[2] APN/CD13 is target for NGR peptide[24]

Table II

Quantitation of the infectivity of H−C− peptide targeted viruses on various tumor cell lines.

	HT1080		MDA-MB-435s		CHO K1		ES-2	
Peptide	**Luciferase**[1,3]	**DNA**[2,3]	**Luciferase**	**DNA**	**Luciferase**	**DNA**	**Luciferase**	**DNA**
RGD	2.3	2.7	1.3	2.8	1.0	1.5	1.1	1.8
NGR	16	1.9	0.3	1.0	0.3	1.4	0.4	0.8
ASL	14	3.3	9.7	1.0	3.5	1.6	8.2	2.5

[1] Luciferase activity of the targeted virus was compared to the detargeted control by fitting a power function to the data (as shown in Figure 1 and Supplementary Figure 2), and is expressed as the fold decrease in titer required to achieve equivalent luciferase activity. Values for all cell lines are the average of two independent experiments.

[2] DNA content of the transduced cells was quantified by real time PCR and the fraction of input virus bound and internalized by cells was determined. The result is expressed as a multiple or fraction of the infectivity of the detargeted control.

[3] DNA values for HT1080 cells are the average of two independent experiments.

Table III

Quantitation of the infectivity of H+C+ peptide targeted viruses on various tumor cell lines.

	HT1080		MDA-MB-435s		CHO K1		ES-2	
Peptide	**Luciferase**[1,3]	**DNA**[2,3]	**Luciferase**[4]	**DNA**	**Luciferase**	**DNA**	**Luciferase**	**DNA**
RGD	2.6	4.1	19	4.4	18	17	42	36
NGR	3.1	1.8	3.1	1.0	2.0	1.7	16	8.9
ASL	4.3	2.5	5.0	1.0	5.5	1.8	12	4.2

[1] Luciferase activity of the targeted virus was compared to the wild type control by fitting a power function to the data (as shown in Figure 1 and Supplementary Figure 2), and is expressed as the fold decrease in titer required to achieve equivalent luciferase activity.

[2] DNA content of the transduced cells was quantified by real time PCR and the fraction of input virus bound and internalized by cells was determined. The result is expressed as a multiple of the infectivity of the wild type control vector.

[3] Values for HT1080 cells are the average of three independent experiments.

[4] Values are the average of two independent experiments.

Table IV

Quantitation of the infectivity of RGD peptide targeted viruses on tumor cell lines using various vector platforms.

	HT1080		MDA-MB-435s		CHO K1		ES-2	
Vector Platform	**Luciferase[1]**	**DNA[2]**	**Luciferase**	**DNA**	**Luciferase**	**DNA**	**Luciferase**	**DNA**
H−C−	1.5	1.7	1.9	2.0	0.5	1.7	1.1[3]	1.8[3]
H−C+	0.03	0.7	1.0	4.2	1.1	3.8	0.4	1.4
H+C−	1.1	7.4	0.3	8.8	0.6	0.2	0.9	0.8
H+C+	2.6	0.5	60	5.1	34	7.7	42[3]	36[3]

[1] Luciferase activity of the RGD targeted virus was compared to the control by fitting a power function to the data shown in Figure 2 and Supplementary Figure 3, and is expressed as the fold decrease in titer required to achieve equivalent luciferase activity.

[2] DNA content of the transduced cells was quantified by real time PCR and the fraction of input virus bound and internalized by cells was determined. The result is expressed as a multiple (or fraction) of the infectivity of the control vector.

[3] same data as shown in Tables II and III as experiments on this cell line were not repeated.